Use of laboratory data to confirm yield and liquefied strength ratio concepts

Scott M. Olson and Timothy D. Stark

Abstract: A laboratory database of triaxial compression test results was collected to examine the use of strength ratios for liquefaction analysis. Specifically, the database was used to: (*i*) validate the yield strength ratio concept (or yield friction angle); (*ii*) demonstrate the parallelism of the consolidation line and steady state line of many sandy soils; and (*iii*) validate the liquefied strength ratio concept. The yield strength ratio of contractive sandy soils in triaxial compression ranges from approximately 0.29 to 0.42 (corresponding to yield friction angles of 16°–23°), while the yield strength ratio from flow failure case histories (which correspond approximately to direct simple shear conditions) ranges from 0.23 to 0.31 (or yield friction angles of 13°–17°). As expected, the yield friction angle is greatest in triaxial compression, smaller in direct simple shear, and likely smallest in triaxial extension. The steady state line and consolidation line of many contractive sandy soils are parallel for a wide range effective stresses, steady state line slopes, fines contents, and grain sizes and shapes that are applicable to many civil engineering structures. As such, the liquefied strength ratio is a constant for many sandy soils deposited in a consistent manner. The liquefied strength ratio is inversely related to state parameter and ranges from approximately 0.02 to 0.22 in laboratory triaxial compression tests. Flow failure case histories fall near the middle of this range.

Key words: liquefaction, liquefied shear strength, yield shear strength, collapse surface, steady state line, penetration resistance.

Résumé : Une base de données de résultats d'essais de compression triaxiale en laboratoire a été colligée pour examiner l'utilisation des rapports de résistance pour l'analyse de la liquéfaction. Spécifiquement, la base de données a été utilisée pour: (*i*) valider le concept de rapport de résistance à la limite élastique (ou l'angle de frottement à la limite élastique); (*ii*) démontrer le parallélisme de la ligne de consolidation et de la ligne d'état permanent de plusieurs sols sableux; et (*iii*) valider le concept du rapport de résistance liquéfiée. Le rapport de la résistance à la limite élastique des sols sableux contractants en compression triaxiale s'étendent d'environ 0,29 à 0,42 (correspondant à des angles de rottement à la limite élastique de 16° à 23°), alors que les rapports de résistance à la limite élastique pour les histoires de cas de rupture en écoulement (qui correspondent approximativement aux conditions de cisaillement direct simple) varient de 0,23 à 0,31 (soit des angles de frottement à la limite élastique de 13° à 17°). Comme prévu, l'angle de frottement à la limite élastique est plus élevé en compression triaxiale, plus faible en cisaillement direct simple, et vraisemblablement la plus faible en extension triaxiale. La ligne d'état permanent et la ligne de consolidation de plusieurs sols sableux contractants sont parallèles pour une large plage de contraintes effectives, de pentes de la ligne d'état permanent, de teneurs en particules fines, de grosseurs et de formes de grains qui sont applicables à plusieurs structures d'ingénieur civil. Comme tel, le rapport de résistance liquéfiée est une constante pour plusieurs sols sableux déposés d'une manière conséquente. Le rapport de résistance liquéfié est en relation inverse avec le paramètre d'état et varie d'environ 0,02 à 0,22 dans les essais de compression triaxiale. Les histoires de cas de rupture par écoulement se situent près du milieu de cette plage.

Mots clés : liquéfaction, résistance au cisaillement par liquéfaction, résistance au cisaillement à la limite élastique, surface d'effondrement, ligne d'état permanent, résistance à la pénétration.

[Traduit par la Rédaction]

Introduction

Olson (2001) and Olson and Stark (2003) proposed a yield strength ratio based on liquefaction case history analysis to evaluate the triggering of liquefaction in contractive, sandy soils. The yield shear strength, s_u(yield), is the peak shear strength available during undrained loading of a saturated, contractive soil (Terzaghi et al. 1996). The yield

Received 18 December 2002. Accepted 31 July 2003. Published on the NRC Research Press Web site at http://cgj.nrc.ca on 3 November 2003.

S.M. Olson.[1] URS Corporation, 1001 Highlands Plaza Drive West, Suite 300, St. Louis, MO 63110, U.S.A.
T.D. Stark. Department of Civil and Environmental Engineering, University of Illinois at Urbana–Champaign, Urbana, IL 61801, U.S.A.

[1]Corresponding author (e-mail: scott_olson@urscorp.com).

 doi: 10.1139/T03-058

strength ratio is defined as the yield shear strength normalized by the prefailure vertical effective stress, $s_u(\text{yield})/\sigma'_{vo}$. The yield strength ratio (or collapse surface) concept is relatively well established for a number of individual sands (e.g., Hanzawa 1980; Sladen et al. 1985; Vaid and Chern 1985; Lade 1992, 1993; Ishihara 1993; Sasitharan et al. 1993) but has not been shown to be universally applicable to sandy soils.

Olson (2001) and Olson and Stark (2002) proposed relationships to estimate the liquefied strength ratio, $s_u(\text{LIQ})/\sigma'_{vo}$ (where $s_u(\text{LIQ})$ is the liquefied shear strength), of contractive, sandy soils using normalized cone and standard penetration test (CPT and SPT) resistance. Although gaining acceptance, the liquefied strength ratio concept still has not been accepted to hold for most sandy soils. Recent laboratory testing (e.g., Ishihara 1993; Baziar and Dobry 1995; Vaid and Sivathayalan 1996) shows that the liquefied shear strength of many cohesionless soils is linearly proportional to initial major principal effective stress. The liquefied strength ratio is a function of state parameter (Fear and Robertson 1995; Olson 2001), however, and the liquefied strength ratio is only a constant if the consolidation line parallels the steady state line (Finn 1998; Olson 2001).

As alluded to above, a number of questions arise in applying strength ratios to liquefaction problems. These questions are as follows: (*i*) Is the yield strength ratio concept universally applicable to sandy soils (including silty sands)? (*ii*) Under what conditions are the consolidation line and steady state line of loose (i.e., contractive), sandy soils parallel? (*iii*) Does a unique relationship exist between state parameter and liquefied strength ratio for sandy soils?

This paper attempts to answer these questions using laboratory test data. To this end, Olson (2001) collected and interpreted a database of laboratory test results, primarily triaxial compression tests, from published literature. This paper describes the sands in the database and addresses the issues raised in the previous paragraph. The laboratory data validate the relationships presented by Olson and Stark (2002, 2003) and extend their application beyond the conditions represented by the case history database.

Laboratory database of sandy soils

Soil properties and test results

Table 1 summarizes the laboratory database collected for this study. The table contains grain characteristics, maximum and minimum void ratios, and references for each of the sands studied. Table 2 presents the steady state line parameters and steady state (or constant volume) effective friction angles and compressibility data available for each sand. In Table 2, the slope of the steady state line in $e - \log p'$ space is defined as λ, and the intercept at 1 kPa (sometimes referred to as Γ) is the value of void ratio (e) on the steady state line at a mean effective stress (p') of 1 kPa. Both the one-dimensional compressibility index, C_c, and the slope of the consolidation line during an increase in isotropic confining stress (i.e., slope of the $e - \log p'_{mean}$ line) are reported if available.

A total of 245 triaxial compression tests conducted primarily on reconstituted samples are included in the database. Because of the size of the database, it is not included herein but is available in Olson (2001). The database includes end of consolidation values of void ratio (e_c), relative density (D_r), and state parameter (ψ), and major and minor principal effective stresses after consolidation (σ'_{1c} and σ'_{3c}, respectively) are reported, if available. State parameter, ψ, is defined as the difference between the void ratio at the end of consolidation, e_c, at a given mean effective confining stress and the void ratio at steady state, e_{ss}, for the same mean effective stress. Where applicable, values of state parameter are calculated using the position of the upper flow (UF) line (e.g., Konrad 1990). Values of deviator stress and porewater pressure at yield ($q_u(\text{yield})$ and Δu_{yield}), at the quasi-steady state ($q_u(\text{min})$ and Δu_{min}), and at the steady state (q_{us} and Δu_{ss}) during shear also are reported. The yield and liquefied shear strengths are defined as

$$[1] \qquad s_u(\text{yield}) = \frac{q_u(\text{yield})}{2}$$

and

$$[2] \qquad s_u(\text{LIQ}) = \frac{q_{us}}{2}\cos\phi'_{ss}$$

respectively, where ϕ'_{ss} is the steady state (or constant volume) friction angle reported in Table 2.

Direct simple shear, torsional or rotational shear, and triaxial extension tests are not included in Table 1. The reasons for not including these data in this study are: (*i*) considerably fewer test results using these modes of shear are available in the literature; (*ii*) at small to intermediate strain levels, values of yield and quasi-steady-state shear strength will differ depending on the mode of shear; and (*iii*) the purpose of this study is to confirm the yield and liquefied strength ratio concepts, not to develop correlations for use in design. In addition, only tests conducted at equal all-around pressures (isotropic confining pressures) are included for simplicity and consistency. While anisotropic consolidation stress conditions do not affect the position of the collapse surface or liquefied shear strengths, the magnitudes of yield shear strength are affected.

As discussed by Olson (2001) and Olson and Stark (2002, 2003), the mode of shear for most of the flow failure case histories approximates direct simple shear conditions within the zone of liquefaction. For direct comparison with the field data, laboratory direct simple, torsional, or rotational shear test results would be required. Unfortunately, test results for loose sands using these modes of shear are limited in the literature.

Factors affecting the steady state line slope

The slope of the steady state line is affected by soil gradation, and minor changes in gradation can cause significant changes in the slope of the steady state line (Poulos et al. 1985*a*). Poulos et al. (1985*a*) also stated that increasing grain angularity increases the slope of the steady state line. Fear and Robertson (1995) and Zlatovic and Ishihara (1995) presented data that suggest the slope of the steady state line of a given soil increases with increasing fines content.

Figure 1 catalogs the fines contents and steady state line slopes for the sands in Table 1. Although the addition of

Table 1. Laboratory database of sandy soils used to examine strength ratio concepts.

Sand No.	Sand name	D_{50} (mm)	FC (%)	Void ratio e_{max}	Void ratio e_{min}	References
1	Dune sand (DS)	0.21	3	0.91 (A)	0.54 (A)	Konrad 1990
2	Well-rounded silica sand (WA)	0.175	1	1.06 (A)	0.67 (A)	Konrad 1990
3	Fraser River Delta sand (FRD)	0.25	3–15	1.00 (A)	0.60 (A)	Chillarige et al. 1997
4	Duncan Dam sand (DD)	0.2	6.5	1.15 (—)	0.76 (—)	Pillai and Stewart 1994
5	Hostun RF sand (HRF)	0.38	0	1 (—)	0.656 (—)	Canou et al. 1994
6	Garnet tailings (GT)	0.17	20	1.52 (—)	0.53 (H)	Highter and Tobin 1980; Highter and Vallee 1980
7	Zinc tailings (ZT)	0.2	17	1.43 (—)	0.49 (H)	Highter and Tobin 1980; Highter and Vallee 1980
8	Natural silt (NS)	0.013	98	1.526 (—)	0.434 (—)	Dyvik and Høeg 1999
9	Fine–coarse sand (FCS)	0.33	1	0.796 (—)	0.404 (—)	Dierichs and Forster 1985
10.1	Ottawa banding sand (OBS)[a]	0.19	2	0.82 (—)	0.51 (—)	Dennis 1988
10.2	Ottawa banding sand (OBS)[b]	0.19	2	0.82 (—)	0.51 (—)	Dennis 1988
10.3	Ottawa banding sand (OBS)[c]	0.19	2	0.82 (—)	0.51 (—)	Dennis 1988
10.4	Ottawa banding sand (OBS)[d]	0.19	2	0.82 (—)	0.51 (—)	Dennis 1988
11	Nevada fine sand (NFS)	0.12	—	0.87 (—)	0.57 (—)	Arulanandan et al. 1993
12.1	Nerlerk 0–2% (N2)	0.23–0.28	0–2	0.94 (C)	0.62 (C)	Sladen et al. 1985
12.2	Nerlerk 12% (N12)	0.28	12	0.96 (B)	0.43 (C)	Sladen et al. 1985
13	Leighton Buzzard sand (LBS)	0.86	0	0.75 (C)	0.58 (C)	Sladen et al. 1985
14	Syncrude tailings sand (STS)	0.17	10	0.93 (A)	0.55 (A)	Sladen and Handford 1987
15	Tottori sand (TS)	0.28	0	1.008 (D)	0.638 (D)	Takeshita et al. 1995
16	Monterey #9 sand (M9S)	0.35	0	0.86 (E)	0.53 (I)	Riemer et al. 1990; Riemer and Seed 1992, 1997
17	Sydney sand (SS)	0.3	—	0.855 (—)	0.565 (—)	Chu 1995
18	Arabian Gulf sand (AGS)	—	40	—	—	Hanzawa 1980
19	Hostun RF sand (HRFS)	0.32	0	1 (—)	0.655 (—)	Konrad 1993
20	Till sand (TillS)	0.11	32	0.835 (—)	0.3625 (—)	Konrad 1993
21	Massey Tunnel sand (MTS)	0.25	3	1.102 (F)	0.712 (F)	Konrad and Pouliot 1997
22	Quebec sand (QS)	0.5	0	0.79 (B)	0.54 (F)	Konrad 1998
23	Erksak 330/0.7 (E330)	0.33	0.7	0.753 (—)	0.469 (—)	Been et al. 1991
24	Ottawa sand (C109)	0.34	0	0.82 (A)	0.5 (A)	Sasitharan et al. 1993, 1994
25	Sand F	0.205	0	1.88 (G)	1.23 (G)	Castro and Poulos 1977; Castro 1969
26	Sand B	0.16	0	0.84 (G)	0.5 (G)	Castro and Poulos 1977; Castro 1969
27	Sand C	0.27	1	0.99 (G)	0.66 (G)	Castro and Poulos 1977; Castro 1969
28	Sand H	0.66	13	0.73 (G)	0.36 (G)	Castro and Poulos 1977; Castro 1969
29	Sand A	0.2	2	1.88 (G)	1.23 (G)	Castro 1969
30	Alcan tailings (AT)	0.002	99	—	—	Poulos et al. 1985*b*
31	Mai-Liao sand (MLS)	0.105	15	1.06 (—)	0.59 (—)	Huang et al. 1999
32	Star Morning tailings (SMT)	0.062	51	—	—	Bryant et al. 1983
33	Bunker Hill tailings (BHT)	0.0097	87	—	—	Bryant et al. 1983
34	Coeur Mine tailings (CMT)	0.06	54	—	—	Bryant et al. 1983
35	Galena tailings (GT)	0.086	40	—	—	Bryant et al. 1983
36	Lucky Friday tailings (LFT)	0.065	53	—	—	Bryant et al. 1983
37	Mission tailings (MT)	0.04	60	—	—	Bryant et al. 1983
38	Morenci tailings (MoT)	0.086	47	—	—	Bryant et al. 1983
39	Climax tailings (CT)	0.026	67	—	—	Bryant et al. 1983
40	Lornex Mine tailings (LMT)	0.256	7	—	—	Bryant et al. 1983
41	Ottawa sand F125 (F125)	0.1	12	—	—	Vasquez-Herrera and Dobry 1989
42	Sand A (SA)	0.15	13	—	—	Baziar and Dobry 1995
43	San Fernando SF7 sand (SF7)	0.075	50	0.72 (—)	0.34 (—)	Baziar and Dobry 1995; Seed et al. 1989

Table 1 (*concluded*).

Sand No.	Sand name	D_{50} (mm)	FC (%)	Void ratio e_{max}	Void ratio e_{min}	References
44	Toyoura sand (ToS)	0.17	0	0.977 (D)	0.597 (D)	Ishihara 1993
45	Lagunillas sandy silt (LSS)	0.05	74	1.389 (D)	0.766 (D)	Ishihara 1993
46	Tia Juana silty sand (TJSS)	0.16	12	1.099 (D)	0.62 (D)	Ishihara 1993

Note: Maximum (e_{max}) and minimum (e_{min}) void ratios were determined using the following methods as indicated in parentheses: A, ASTM D2049-69 (as reported by investigators); B, Kolbuszewski 1948; C, unspecified ASTM procedure; D, Japanese Society of Soil Mechanics and Foundation Engineering; E, dry pluviation; F, ASTM D4254 (as reported by investigators); G, nonstandard procedure; H, modified Proctor compaction; I, modified Japanese method. D_{50}, median grain diameter; FC, fines content; —, not available.

[a]Strain control, equal energy.
[b]Strain control, equal volume.
[c]Stress control, equal energy.
[d]Stress control, equal volume.

Fig. 1. Catalog of fines contents and steady state line slopes for sandy soils in laboratory database.

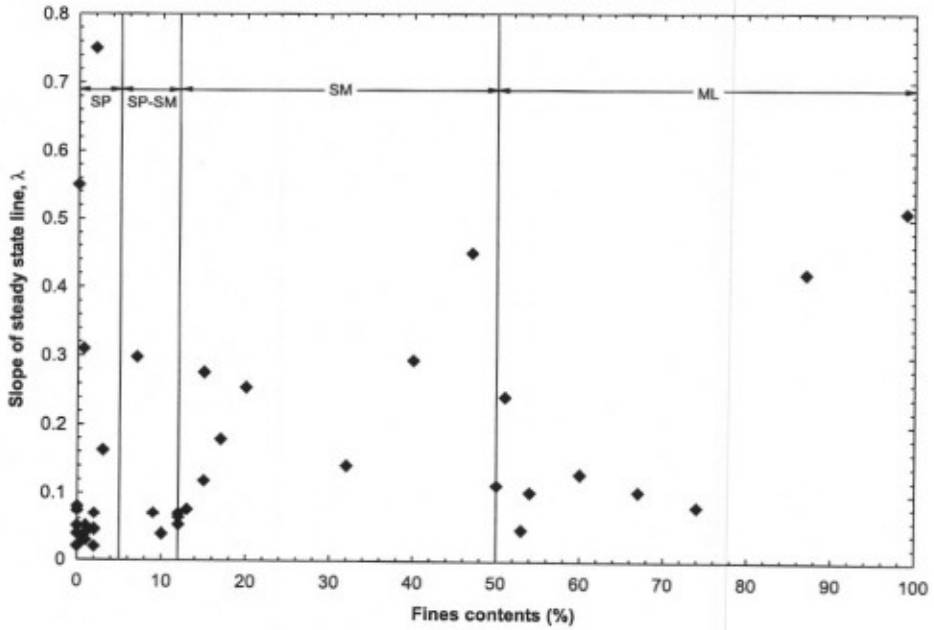

fines to a given sand may increase the slope of the steady state line, Fig. 1 indicates no general trend between the slope of the steady state line and increasing fines content. These data indicate that grain angularity may affect the slope of the steady state line at least as significantly as fines content, as the soil in the laboratory database with the steepest steady state line is an angular clean sand (sand A).

Confirmation of yield strength ratio concept

As discussed by Olson and Stark (2003), Hanzawa et al. (1979) indicated that peak shear strengths measured during shear tests produced an approximately linear peak shear strength envelope in stress path space. Sladen et al. (1985) defined a collapse surface in three-dimensional void ratio – shear stress – effective normal stress space to represent conditions that would lead to the triggering of flow liquefaction, or strain-softening behavior. The collapse surface represents the locus of peak (or yield) shear stresses that a given soil can reach for varying combinations of void ratio and normal effective stress. A number of other investigators (e.g., Vaid and Chern 1983, 1985; Kramer and Seed 1988; Vasquez-Herrera and Dobry 1989; Lade 1992, 1993; Ishihara 1993; Konrad 1993; Sasitharan et al. 1993, 1994; among others) identified similar yield conditions and proposed various names for these conditions. Figure 2 presents an example of the collapse surface (or peak strength envelope) in normalized stress path space for Hostun RF sand (see Tables 1 and 2 for details).

Olson (2001) termed this line of yield (or peak) shear strengths the yield strength envelope because it defines the stress conditions at which the yield shear strength is mobilized. Direct comparisons of yield conditions defined in stress path space (p'–q, where q is the deviator stress), Mohr–Coulomb space (shear stress-effective normal stress), and other conditions can be made by known trigonometric conversions.

Table 2. Steady state and compressibility parameters of sandy soils in laboratory database.

Sand No.	Sand name	Steady state data			Compressibility		
		Slope, λ	Intercept at 1 kPa	ϕ'_{ss} (°)	C_c	Isotropic	Effective stress range (kPa)
1	Dune sand (DS)	0.1625	1.1521	34.4	—	0.103	50–3000
2	Well-rounded silica sand (WA)	0.02932	1.0095	34	—	—	—
3	Fraser River Delta sand (FRD)	0.07	1.11	30	0.27	0.12	<800
4	Duncan Dam sand (DD)	—	—	—	0.15	—	100–1500
5	Hostun RF sand (HRF)	—	—	33.4	—	—	—
6	Garnet tailings (GT)	0.255	1.59	—	—	—	—
7	Zinc tailings (ZT)	0.179	1.3275	—	—	—	—
8	Natural silt (NS)	—	—	36	—	—	—
9	Fine–coarse sand (FCS)	—	—	—	—	—	—
10.1	Ottawa banding sand (OBS)[a]	0.069	0.900	30	—	—	—
10.2	Ottawa banding sand (OBS)[b]	0.0453	0.856	30	—	—	—
10.3	Ottawa banding sand (OBS)[c]	0.0447	0.849	30	—	—	—
10.4	Ottawa banding sand (OBS)[d]	0.0199	0.789	30	—	—	—
11	Nevada fine sand (NFS)	0.0657	0.832	29.1	—	—	—
12.1	Nerlerk 0–2% (N2)	0.04	0.883	30	—	—	—
12.2	Nerlerk 12% (N12)	0.07	0.80	31	—	—	—
13	Leighton Buzzard sand (LBS)	0.08	1.00	30	—	—	—
14	Syncrude tailings sand (STS)	0.039	0.845	29.7	—	0.039	100–1200
		0.039			—	0.01	5–100
15	Tottori sand (TS)	—	—	35.5	—	0.02	50–1000
16	Monterey #9 sand (M9S)	—	—	32.3	—	—	—
17	Sydney sand (SS)	—	—	31	—	—	—
18	Arabian Gulf sand (AGS)	—	—	—	—	—	—
19	Hostun RF sand (HRFS)	0.0735	1.0546	33.4	—	—	—
20	Till sand (TillS)	0.1415	0.791	34.6	—	—	—
21	Massey Tunnel sand (MTS)	—	—	39	—	—	—
22	Quebec sand (QS)	0.021	0.757	—	—	—	—
23	Erksak 330/0.7 (E330)	0.0306	0.820	30	—	—	<1000
		0.310	1.167		—		>1000
24	Ottawa sand (C109)	0.0387	0.864	30.6	—	—	—
25	Sand F	0.55	—	—	0.46	—	50–1000
26	Sand B	0.05	0.804	30	0.03	—	10–1000
27	Sand C	0.05	1.005	35	0.037	—	<300
28	Sand H	0.076	—	—	0.074	—	100–400
29	Sand A	0.75	—	38	0.56	—	>100
30	Alcan tailings (AT)	0.51	—	32.9	0.514	—	10–100
		0.51	—		0.47	—	100–200
31	Mai-Liao sand (MLS)	0.119	—	31.6	0.153	—	<200
		0.276	—		0.27	—	>200
32	Star Morning tailings (SMT)	0.242	—	—	0.216	—	<10
		RP[e]			0.076	—	>10
33	Bunker Hill tailings (BHT)	0.42	—	—	0.394	—	<4
		RP[e]			0.098	—	>4
34	Coeur Mine tailings (CMT)	0.103	—	—	0.07	—	>10
35	Galena tailings (GT)	0.294	—	—	0.144	—	<3
		RP[e]			0.042	—	>3
36	Lucky Friday tailings (LFT)	0.046	—	—	0.046		>3
37	Mission tailings (MT)	0.13	—	—	0.127	—	>10
38	Morenci tailings (MoT)	0.45			0.395	—	<5
		RP[e]			0.136	—	>5
39	Climax tailings (CT)	0.104	—	—	0.104	—	>3
40	Lornex Mine tailings (LMT)	0.160	—	34.8	0.079	—	50–200
		0.32	—		0.183	—	200–1000
41	Ottawa sand F125 (F125)	0.052	0.881	33.7	—	—	—
42	Sand A (SA)	—	—	33.7	—	—	—

Table 2 (*concluded*).

Sand No.	Sand name	Steady state data			Compressibility		Effective stress range (kPa)
		Slope, λ	Intercept at 1 kPa	ϕ'_{ss} (°)	C_c	Isotropic	
43	San Fernando SF7 sand (SF7)	0.113	—	33.7	—	0.146	20–100
44	Toyoura sand (ToS)	0.02	—	31	—	0.03	50–600
45	Lagunillas sandy silt (LSS)	0.082	—	31	—	0.099	50–300
46	Tia Juana silty sand (TJSS)	0.063	—	30.5	—	0.073	50–400

Note: —, not available.
[a]Strain control, equal energy.
[b]Strain control, equal volume.
[c]Stress control, equal energy.
[d]Stress control, equal volume.
[e]Reported to be approximately parallel to compressibility (C_c) by investigators for this effective stress range.

Fig. 2. Summary of undrained triaxial compression test results for Hostun RF sand presented in normalized stress space (after Konrad 1993). M_F, slope of failure envelope in p'–q space.

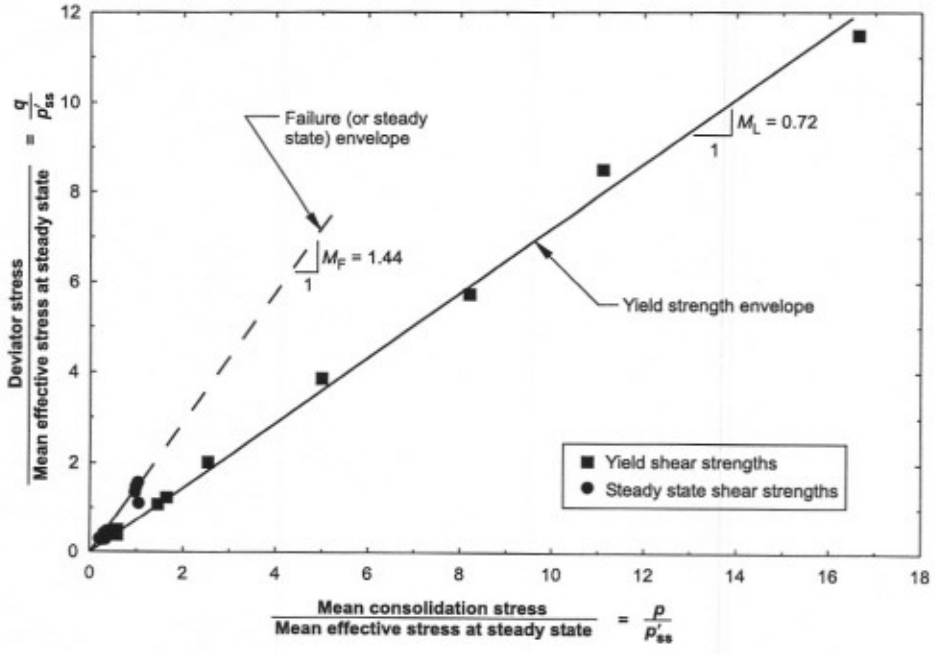

Collapse surface from laboratory data

The laboratory database was classified using the Unified Soil Classification System as clean sands (SP, less than 5% fines), clean sands to silty sands (SP–SM, between 5% and 12% fines), silty sands (SM, between 12% and 50% fines), and sandy silts to silts (ML, greater than 50% fines). Figure 3 presents collapse surface data in p'–q space for the clean sands (SP) in the laboratory database. The slope of the collapse surface in p'–q space often is referred to as M_L. The slope M_L can be related to a Mohr–Coulomb effective friction angle at yield, ϕ_y, as follows:

$$[3] \qquad \sin\phi_y = \frac{3M_L}{6 + M_L}$$

As indicated by Olson and Stark (2003), the tangent of the yield friction angle is approximately equivalent to the yield strength ratio.

Referring to Fig. 3, the slope of the collapse surface in triaxial compression ranges from approximately 0.62 to 0.90 for nearly all the clean sands. Note that the slope of 0.90 has an apparent intercept on the q axis of approximately 55 kPa. At values of mean effective stress, p', less than 700 kPa, the upper bound value of M_L can be approximated as 1.0. These values of collapse surface slope correspond to yield friction angles of 16°–23° (with a maximum value of 25° at mean effective stresses less than 700 kPa).

Figure 4 presents collapse surface data for the clean sands to silty sands (SP–SM) in the laboratory database. For two of these sands, individual data that could be used to evaluate the slope of the collapse surface were not presented. However, the investigators did provide measured values of M_L. These data are plotted in Fig. 4 as dashed lines over the applicable range of mean effective stresses. The SP–SM data in Fig. 4, in general, plot within the upper and lower bound collapse surface values determined for clean sands.

Fig. 3. Summary of yield strength data for clean sands (SP) in laboratory database. Sand names as in Table 1. σ_1' and σ_3', major and minor principal effective stress, respectively.

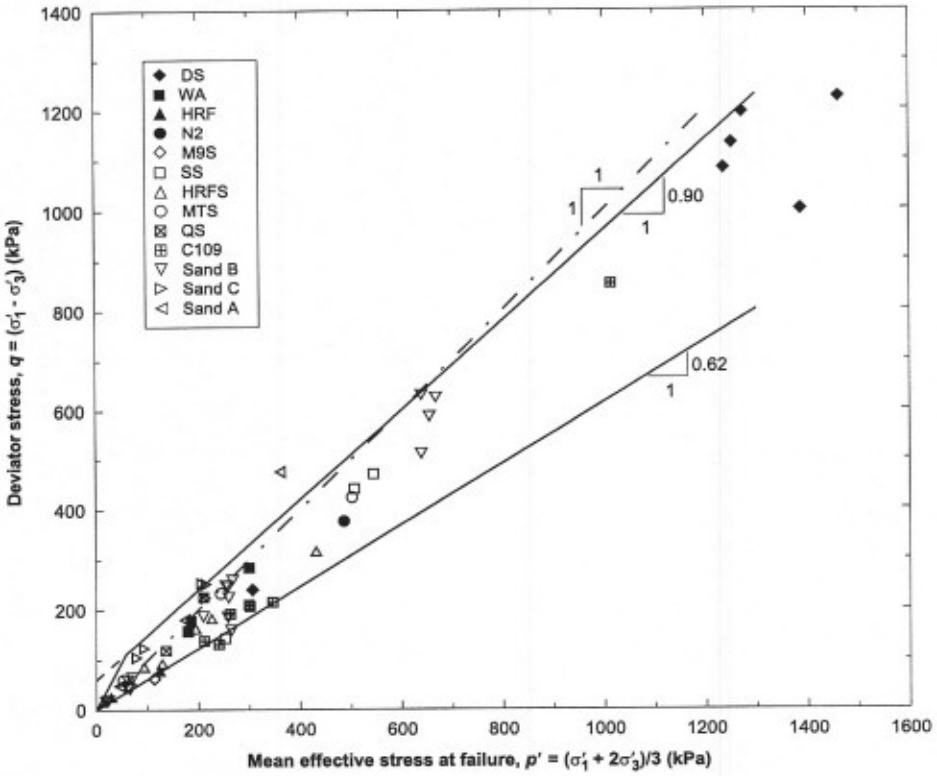

Fig. 4. Summary of yield strength data for clean sands to silty sands (SP–SM) in laboratory database. Sand names as in Table 1.

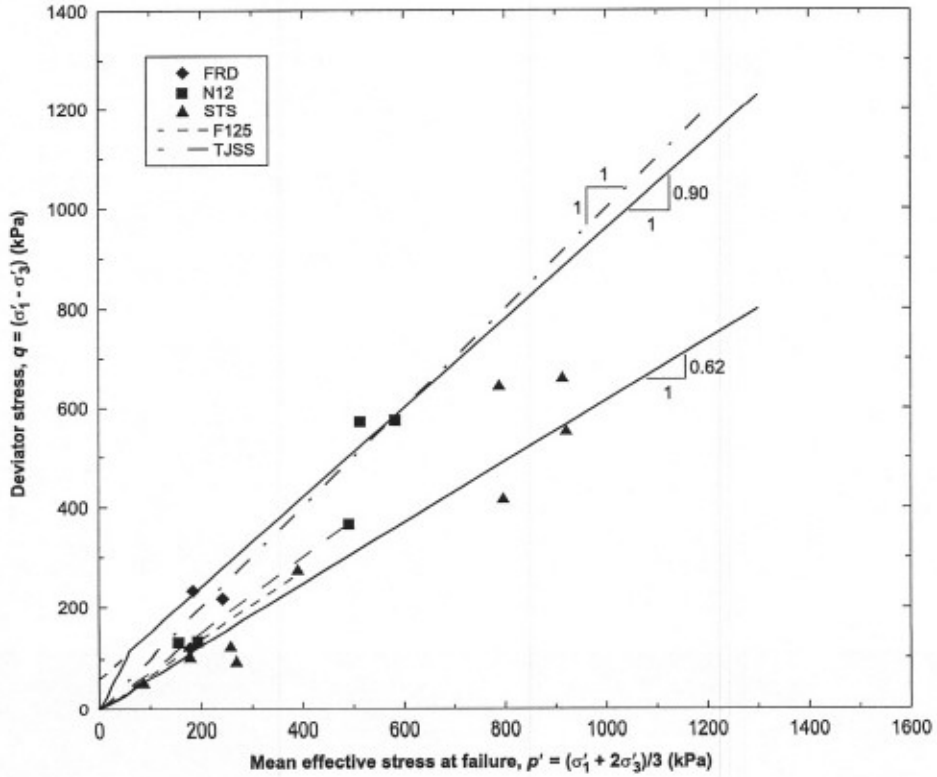

Fig. 5. Summary of yield strength data for silty sands, sandy silts, and silts (SM and ML) in laboratory database. Sand names as in Table 1.

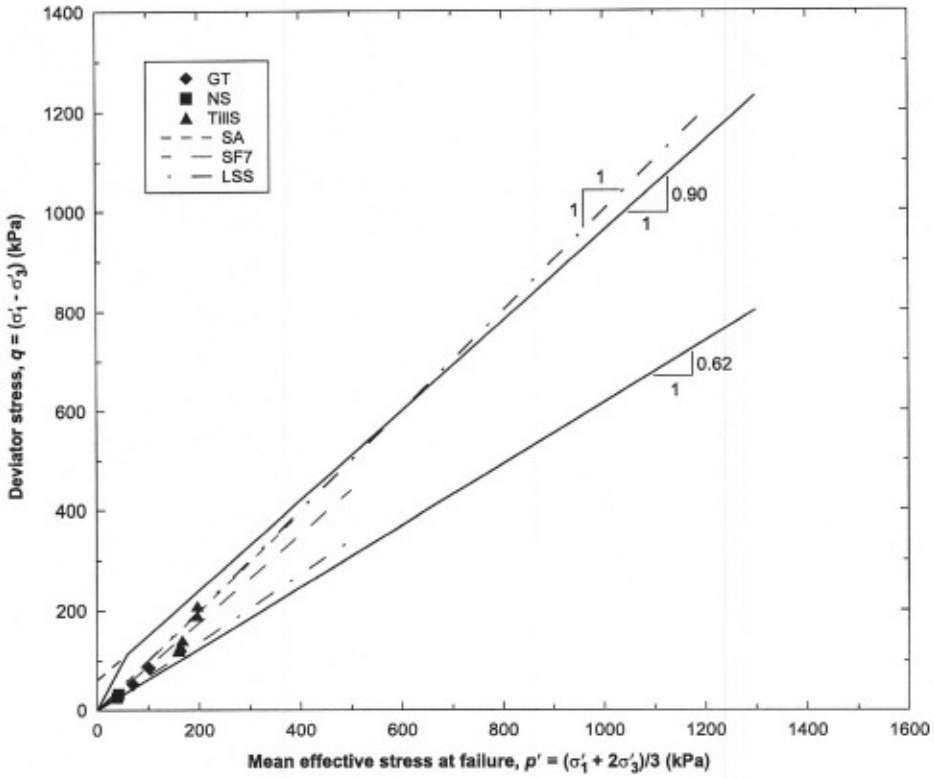

Similarly, Fig. 5 presents collapse surface data for the silty sands, sandy silts, and silts (SM and ML) in the laboratory database. In three cases, investigators reported M_L values rather than individual test results. These M_L data were plotted over the range of applicable mean effective stresses. Again, the SM and ML data plot within the upper and lower bound collapse surface values determined for clean sands.

In summary, the collapse surface slope in triaxial compression for many sandy soils ranges from 0.62 to 0.90 (with an upper bound of 1.0). This corresponds to a range of yield friction angles of 16°–23° (with an upper bound of 25°). In turn, this corresponds to yield strength ratios ranging from 0.29 to 0.42 (with an upper bound of 0.47). The authors anticipate that values of yield strength ratio determined for triaxial compression should be greater than values determined for direct simple shear, which should be greater than values determined for triaxial extension.

Relation between yield strength ratio and state parameter

To clarify the range of potential yield strength ratios determined for triaxial compression, we attempted to correlate yield strength ratio with state parameter. Figure 6 plots values of collapse surface slope against state parameter. Only sands with more than three test results are plotted so that trends could be evaluated reasonably.

As indicated in Fig. 6, there is no unique relation between the slope of the collapse surface and state parameter. For individual sands, however, a general trend of increasing collapse surface slope with decreasing state parameter is observed. This suggests that increases in yield strength ratio correspond to decreases in state parameter. In other words, the yield friction angle increases with increasing density at a given effective stress. Unfortunately, the data are too limited to confirm any possible correlation. It is possible that an alternate definition of state (such as the state index (Ishihara 1993)), excess pore-water pressure ratio at steady state (Yoshimine and Ishihara 1998), or excess pore-water pressure ratio at yield) may provide a better correlation with yield strength ratio.

Comparison of laboratory collapse surface with field data

Figure 7 presents a comparison of the range of collapse surface determined for laboratory triaxial compression test results with the equivalent range of yield strength ratios determined from static flow failure case histories by Olson and Stark (2003). The yield strength ratios determined from static flow failure case histories ranged from about 0.23 to 0.31. This corresponds to yield friction angles of 13°–17° and collapse surface slopes of approximately 0.49–0.65 (using eq. [2]). Mean effective stresses at yield for the case history bounds were computed by assuming a coefficient of earth pressure at rest (K_0) of 0.5.

As expected, the field case history bounds plot slightly below the laboratory bounds. That result is expected because the laboratory bounds correspond to triaxial compression, whereas the field case history bounds correspond approximately to direct simple shear conditions. At small strains, the mobilized shear strength is a function of the mode of

Fig. 6. Relation between state parameter and slope of collapse surface in q–p' space for several sands in laboratory database. Sand names as in Table 1.

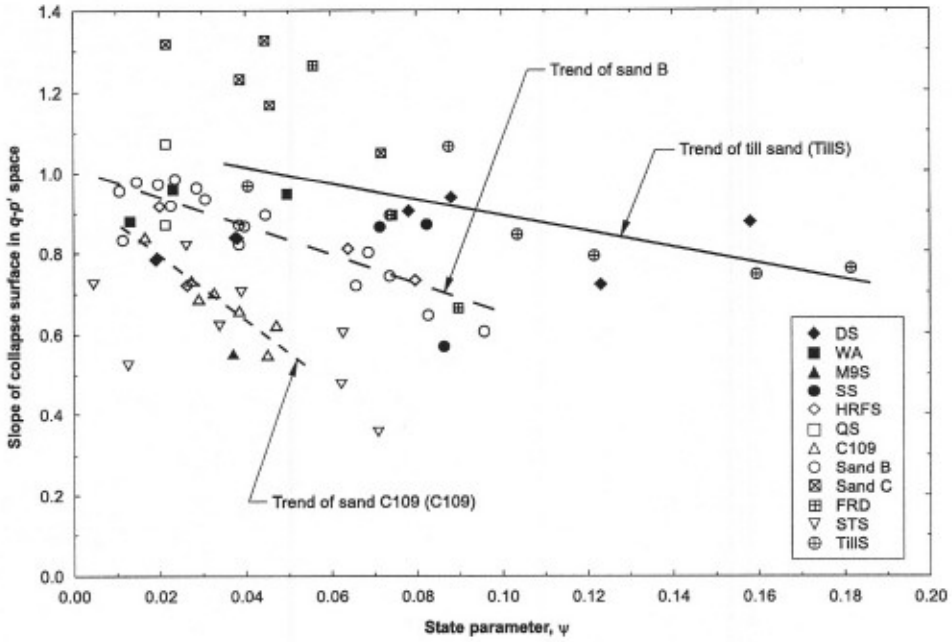

Fig. 7. Comparison of yield strength envelope data (in stress path space) from laboratory database and static flow failure case histories.

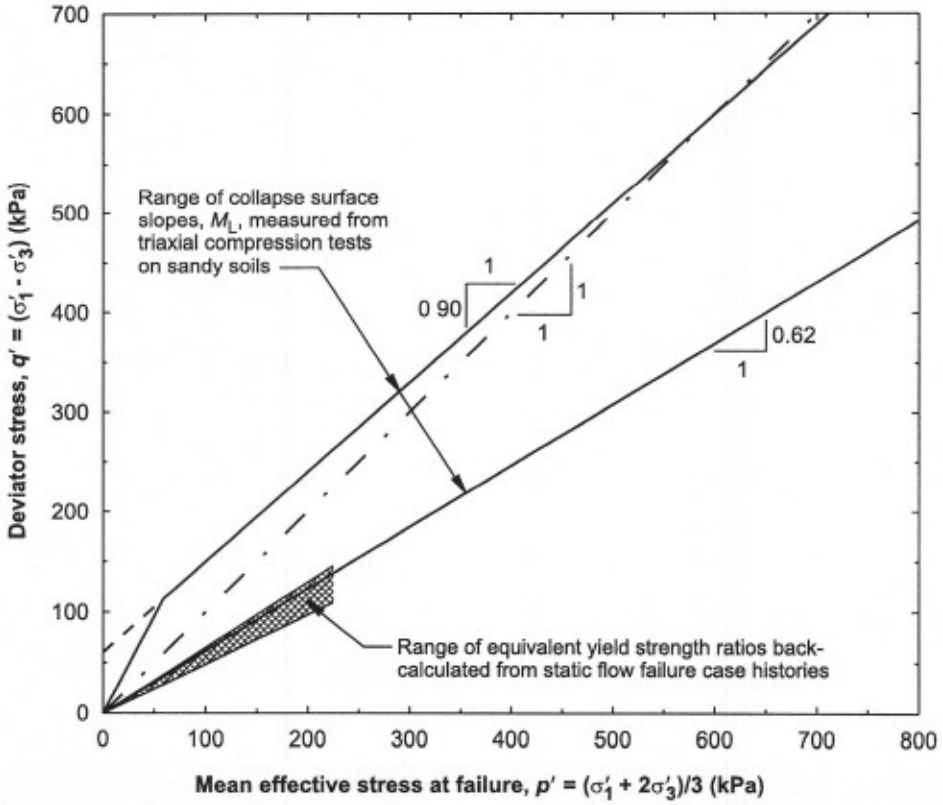

Fig. 8. Comparison of consolidation line and steady state line for remolded layered specimens of silty sand, batch 7, Lower San Fernando Dam (after Baziar and Dobry 1995).

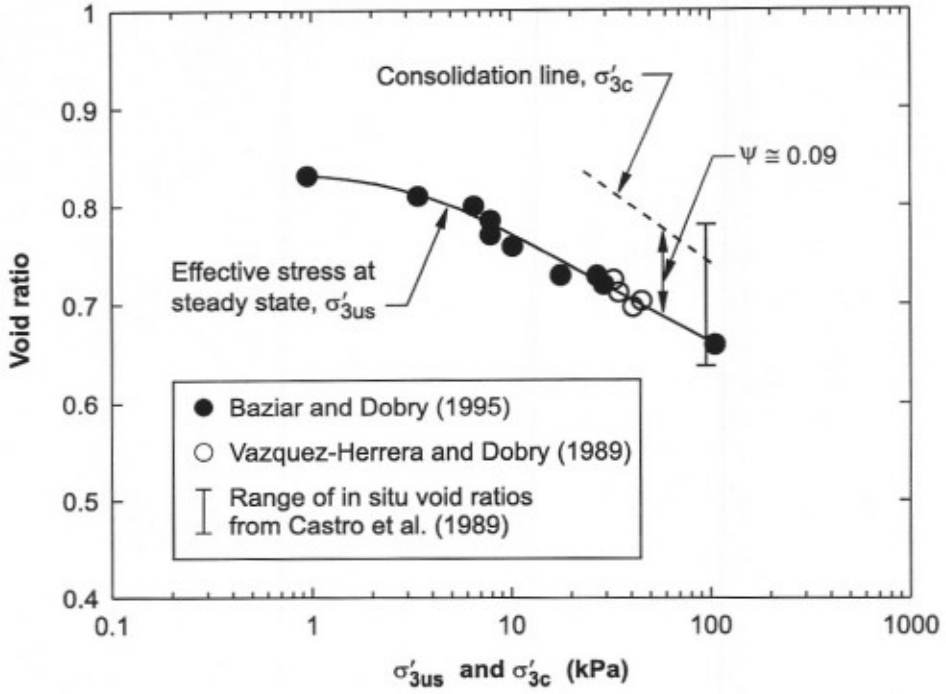

shear, with yield shear strengths being largest in triaxial compression, smaller in direct simple shear, and smallest in triaxial extension. The authors anticipate that triaxial extension collapse surfaces would plot slightly below the field case history bounds.

No attempts were made to relate laboratory yield strength ratio to corrected penetration resistance, because no unique relationship exists between the slope of the collapse surface and state parameter for the laboratory database. However, the agreement among collapse surface data for all sandy soils in the laboratory database (Figs. 3–5) suggests that the yield strength ratio concept is valid. Furthermore, the field data agree with expected laboratory behavior.

Parallelism of steady state line and soil compressibility

As discussed by Olson (2001) and Olson and Stark (2002), when the steady state line parallels the consolidation line, the state parameter and thus the liquefied strength ratio is constant. Figure 8 presents an example of parallelism of the slope of the steady state line and consolidation line for Lower San Fernando Dam silty sand (batch 7). For many sandy soils, the slopes of the steady state line and consolidation line are generally parallel, at least for a given range of effective stresses (Olson 2001). The question then becomes: under what conditions (fines content, stress range, etc.) is it reasonable to assume a parallel steady state line and consolidation line?

Figure 9 presents a comparison of the slopes of the steady state line and consolidation line of the sandy soils in Tables 1 and 2. Table 2 provides the applicable range of effective stress for each sand. It is widely accepted that the consolidation behavior of sands depends on the initial density at deposition. Sands that are deposited in a dense state are less compressible than the identical sand initially deposited in a loose state (e.g., Ishihara 1993). Because liquefaction only occurs in contractive sandy soils, the slopes of the consolidation lines reported in Table 2 were obtained from specimens deposited in initially loose states. As the fines content of the soil increases, the range of initial densities for different depositional procedures tends to decrease. Therefore, differences in compressibility appear to decrease with increasing fines content.

The data in Fig. 9 suggest that for many sandy soils (with a large range of steady state line slopes, fines contents, and grain sizes and shapes) the slopes of the steady state line and consolidation line generally are parallel. Therefore, the liquefied strength ratio generally is a constant for a given soil deposited in a consistent manner. In particular, sandy soils with fines content greater than 12% exhibit nearly parallel slopes of the steady state line and consolidation line. This parallelism holds for a wide range of effective stresses applicable to civil engineering structures, as indicated in Table 2.

In summary, the liquefied strength ratio concept appears valid for many sands, at least over the range of effective stresses applicable to many civil engineering structures. This is particularly true for sandy soils with fines content greater than 12%, which applies to nearly all field cases of flow liquefaction studied by Olson (2001).

Confirmation of liquefied strength ratio concept

As discussed by Olson (2001) and Olson and Stark (2002), recent laboratory testing (e.g., Ishihara 1993; Pillai

Fig. 9. Comparison of consolidation behavior and steady state line slopes for sands in laboratory database.

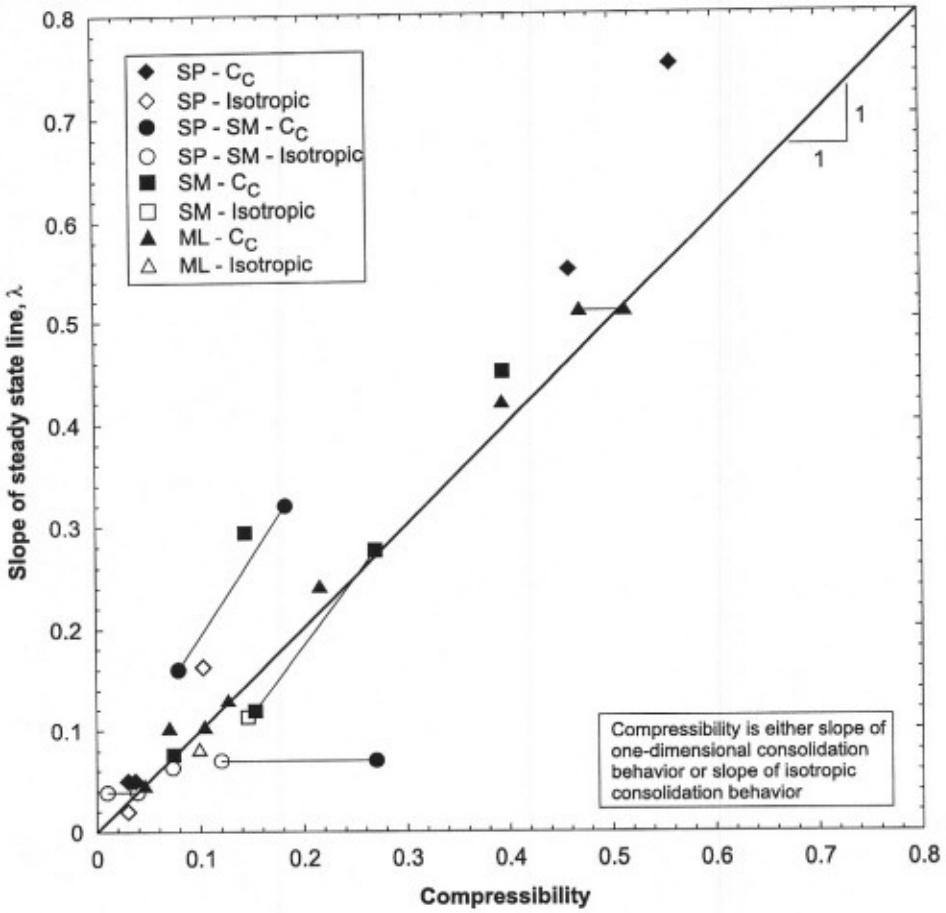

and Salgado 1994; Baziar and Dobry 1995; Vaid and Sivathayalan 1996) shows that the liquefied shear strength of many cohesionless soils is linearly proportional to the initial major principal effective stress. Figure 10 presents an example of this behavior for Lower San Fernando Dam silty sand (batch 7). Fear and Robertson (1995) indicated that for a given method of deposition and mode of shearing, there is a unique value of liquefied strength ratio for a given value of state parameter. A similar example of this relation is shown for Fraser River sand in Fig. 11. Vaid and Sivathayalan (1996) measured liquefied shear strengths over a wide range of void ratios using direct simple shear tests and plotted the resulting liquefied strength ratios versus void ratio after consolidation. An increase in the void ratio at a constant effective consolidation stress in Fig. 11 corresponds to an increase in state parameter. Lastly, relationships between liquefied strength ratio and corrected penetration resistance (e.g., Olson and Stark 2002) assume a relation between decreasing state parameter (or increasing relative density) at a given vertical effective stress and increasing corrected penetration resistance. The following discussion explores the validity of these relations using the laboratory database.

For the following discussion, we use the quasi-steady-state (or minimum) shear strength as the liquefied shear strength, as suggested by Ishihara (1993) and Yoshimine et al. (1999) (among others). The use of the quasi-steady-state rather than the ultimate steady state shear strength may explain the observation by Fear and Robertson (1995) that the relationship between state parameter and liquefied strength ratio depends on the method of deposition and mode of shear. Only contractive sands are susceptible to liquefaction flow failure, however, and for these sands the quasi-steady state and steady state are equivalent (Ishihara 1993; Gutierrez 1998); therefore, it appears reasonable to base the following relations on the minimum shear strength.

Liquefied strength ratio and state parameter

Relationships between minimum (undrained) strength ratio and state parameter are examined for the two sands in the database with sufficient test results, namely sand B (Castro 1969) and Toyoura sand (Ishihara 1993). Figure 12 presents the individual values of minimum shear strength and major principal effective confining stress, σ'_{1c}, for sand B. State parameters for each specimen are shown beside the data points. Contours of equal state parameter were determined by regression analysis. As expected, these data indicate that as state parameter increases (i.e., soil becomes more contractive or looser with respect to the steady state line), the minimum strength ratio decreases.

Figure 13 presents a similar relation between minimum strength ratio and state parameter for Toyoura sand. Although the contours of constant state parameter are not lin-

Fig. 10. Relationship between liquefied shear strength and initial major principal effective stress for remolded layered specimens of silty sand, batch 7, Lower San Fernando Dam (from Baziar and Dobry 1995). K_c, ratio of major to minor principal effective stress after consolidation.

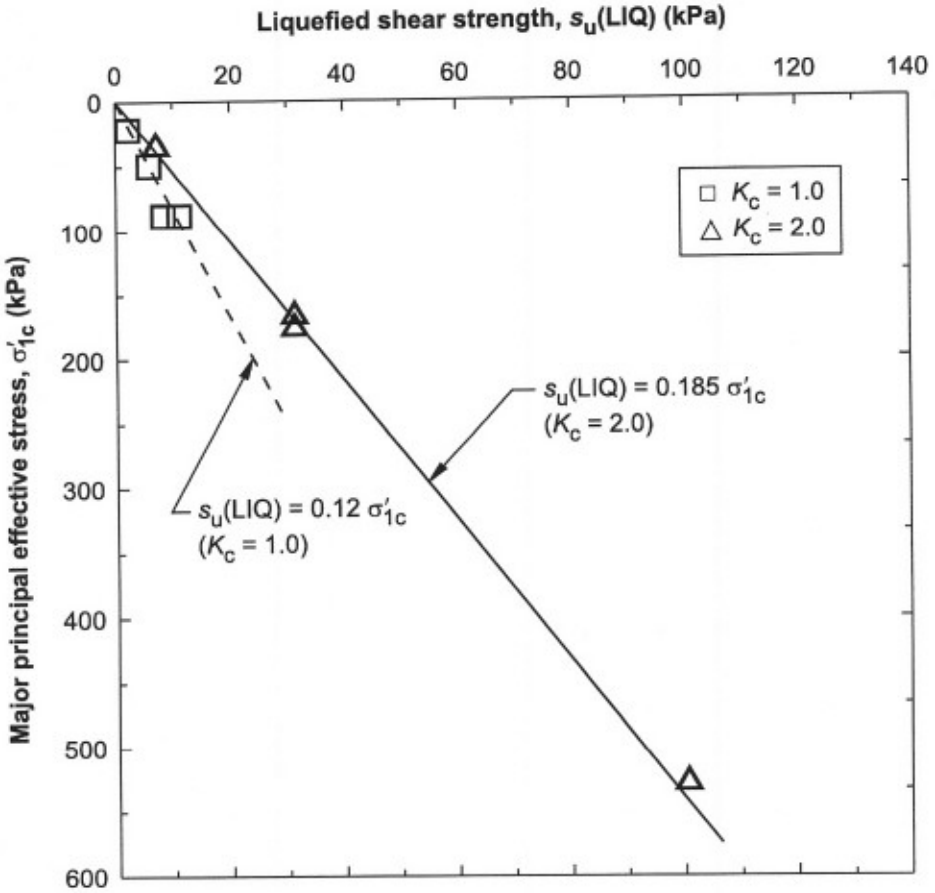

ear, they also indicate that an increase in state parameter corresponds to a decrease in minimum strength ratio.

Figure 14 presents relationships between minimum strength ratio and state parameter for the five sands in the laboratory database with sufficient data to define a clear trend. The trend lines indicate a decrease in the minimum strength ratio with an increase in state parameter. This relation is not unique for all sandy soils, however, because the laboratory minimum strength ratio depends on the slopes of the failure surface (i.e., ϕ'_{ss}) and the steady state line.

Comparison of laboratory minimum strength ratio and field data

Flow failure case histories indicate a trend of increasing liquefied strength ratio with increasing vertical effective stress (Olson and Stark 2002). Figure 15 presents a similar plot for the sands in the laboratory database. Only tests conducted at mean effective stresses less than 1 MPa are included in Fig. 15 because grain crushing often occurs at mean effective stresses greater than 1 MPa (Konrad 1998). Grain crushing significantly increases the slope of the steady state line, and it is not clear whether relations based on state parameter hold when grain crushing occurs.

The data in Fig. 15 indicate that for all sandy specimens with positive values of state parameter (corresponding to specimens initially loose of the steady state line) in the laboratory database, the minimum strength ratio ranges from approximately 0.02 to 0.22. Careful examination of these data indicate that, in general, increasing values of state parameter correspond to decreasing values of liquefied strength ratio for all sands.

For comparison, the liquefaction field case history bounds determined by Olson and Stark (2002) are included in Fig. 15. The field case histories plot within the boundaries of the laboratory data. Direct comparison of the triaxial compression laboratory test data and the field data (corresponding approximately to direct simple shear) is only appropriate, however, if the steady state is independent of the mode of shear. This issue is clouded by limitations of existing laboratory testing equipment. If direct comparison is appropriate, however, it appears that the case history data correspond to laboratory data with state parameters ranging from roughly 0.02 to 0.10.

Laboratory strength ratio and relative density

For eventual comparison to field data, Fig. 16 presents a comparison between relative density and minimum strength ratio for the clean sand laboratory data. Figure 16 includes an upper and lower bound relationship between relative density and minimum strength ratio for clean sands tested in

Fig. 11. Variation of liquefied strength ratio (measured in direct simple shear) with void ratio for Fraser River sand (after Vaid and Sivathayalan 1996).

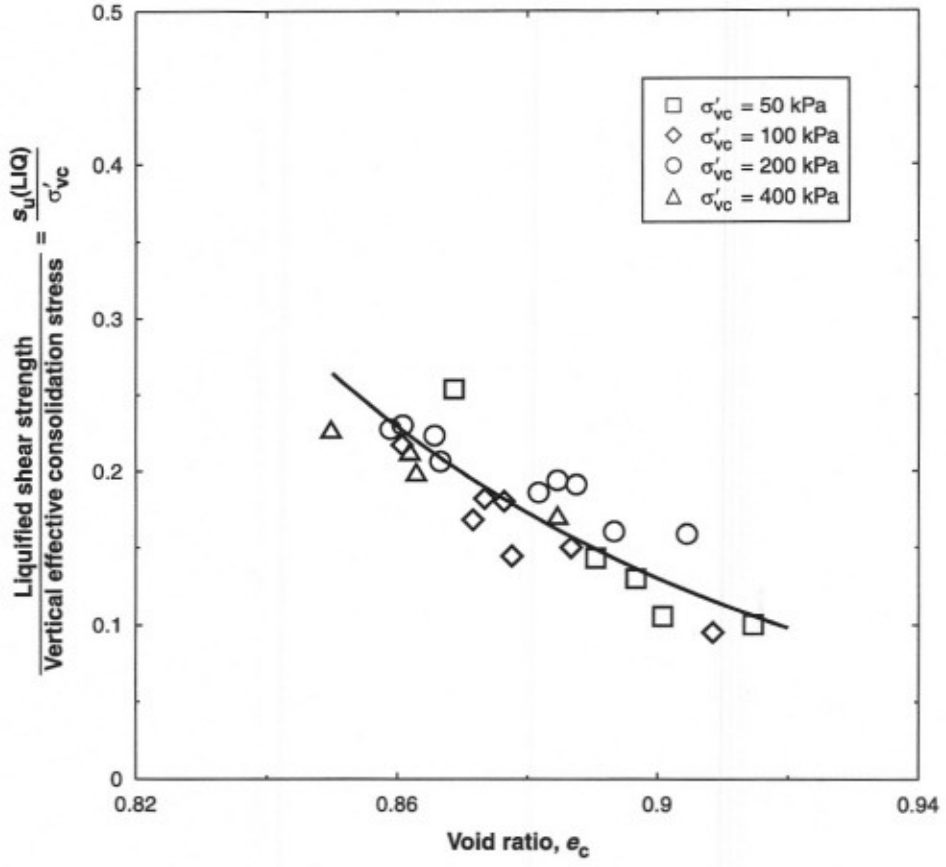

Fig. 12. Relations between liquefied shear strength and major principal effective stress after consolidation for various values of state parameter for sand B (data from Castro 1969).

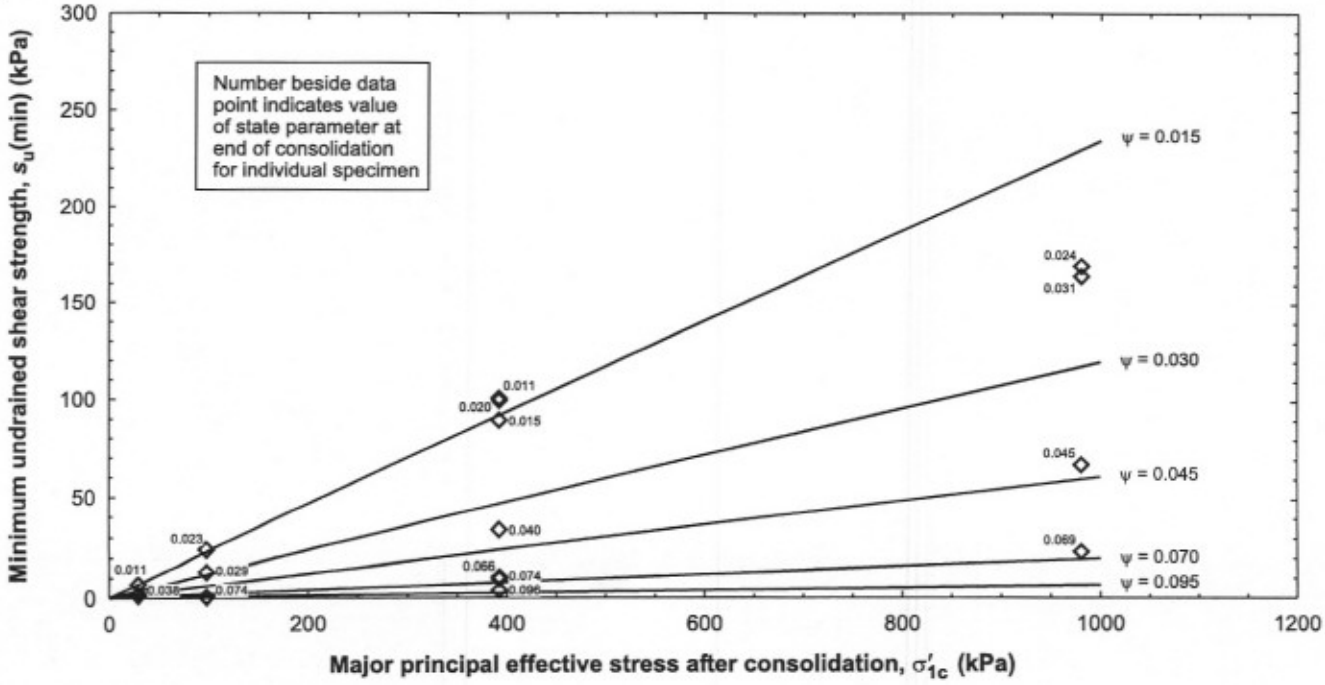

Fig. 13. Relations between liquefied shear strength and major principal effective stress after consolidation for various values of state parameter for Toyoura sand (data from Ishihara 1993).

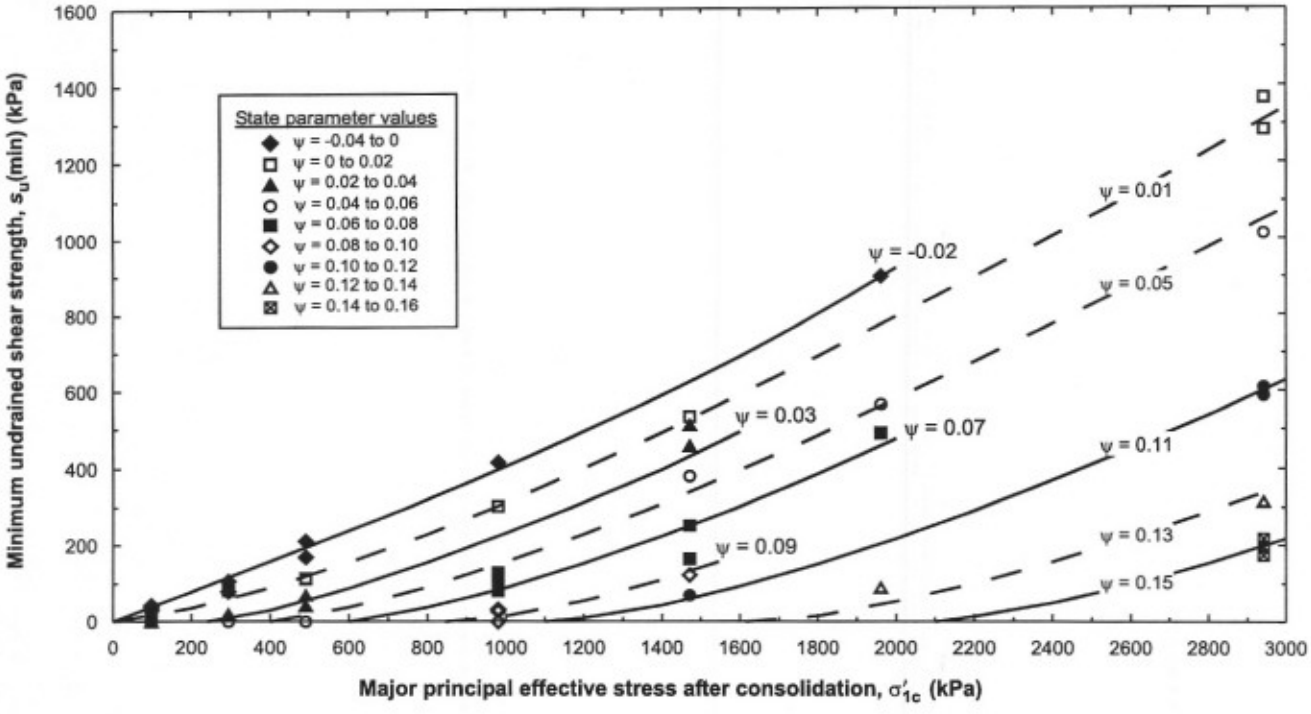

Fig. 14. Relationships between liquefied strength ratio and state parameter for five sands in laboratory database. Sand names as in Table 1.

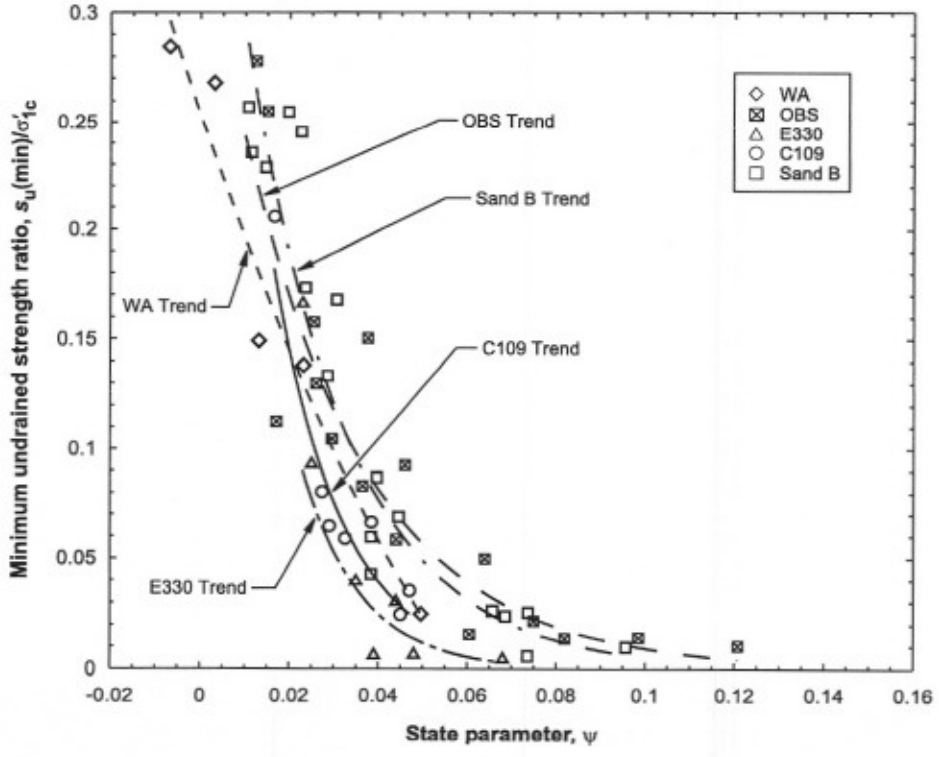

Fig. 15. Comparison of liquefied strength ratio data from laboratory database and flow failure case histories.

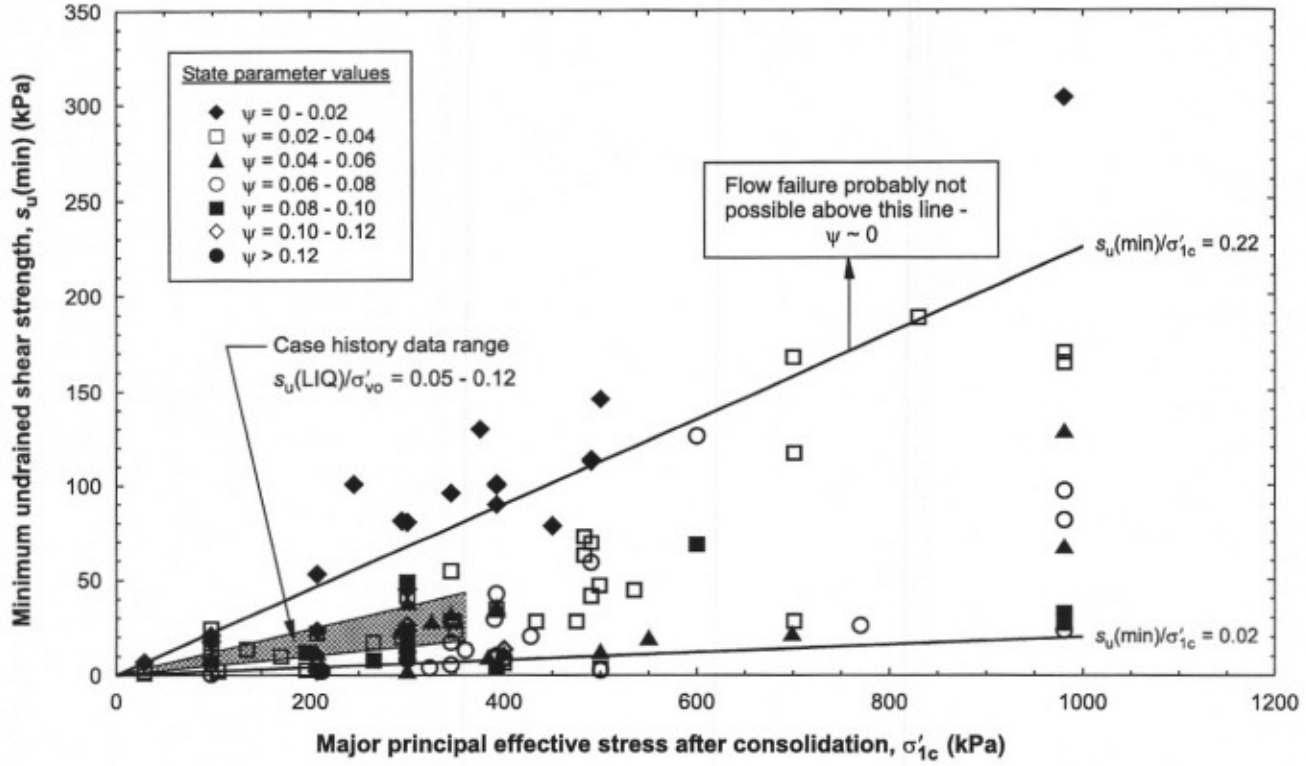

Fig. 16. Relationships between relative density and liquefied strength ratio for clean sands in laboratory database. Sand names as in Table 1.

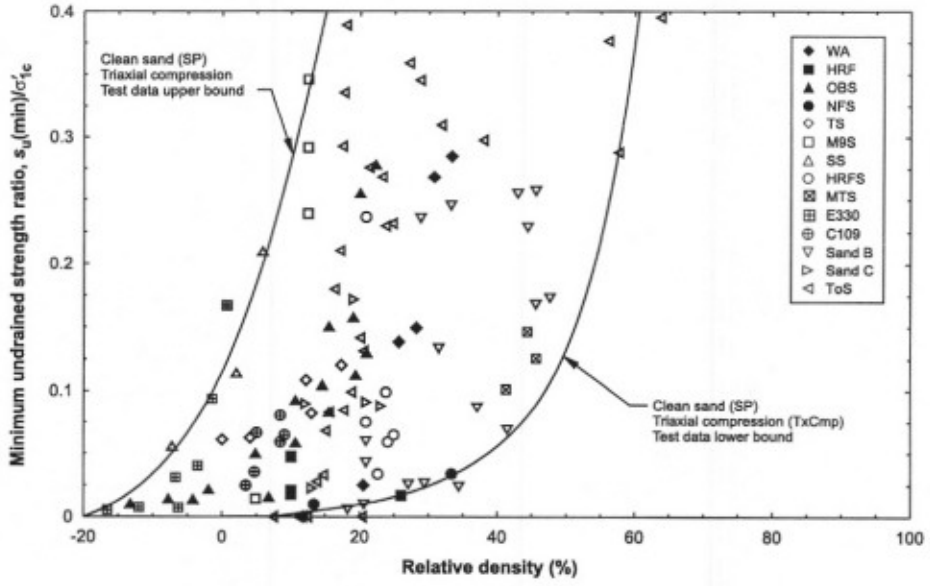

triaxial compression. The lower bound relationship approaches a vertical asymptote at a relative density of approximately 60%. This vertical asymptote of D_r = 60% is similar to those suggested by Thevanayagam et al. (1996*a*, 1996*b*) of approximately 60%–75% for sands with less than 12% fines content.

Figure 17 presents a similar plot of relative density and minimum strength ratio for clean sands to silty sands (SP–SM), silty sands (SM), and sandy silts to silts (ML). The SP–SM data plot above the lower bound relation for clean sands. Therefore, the clean sand bound may be applicable to sands with less than about 12% fines content. In addition, although there are significantly fewer data in this plot, a lower bound relation for silty sands is included based on similar

Fig. 17. Relationships between relative density and liquefied strength ratio for sand soils in laboratory database. Sand names as in Table 1.

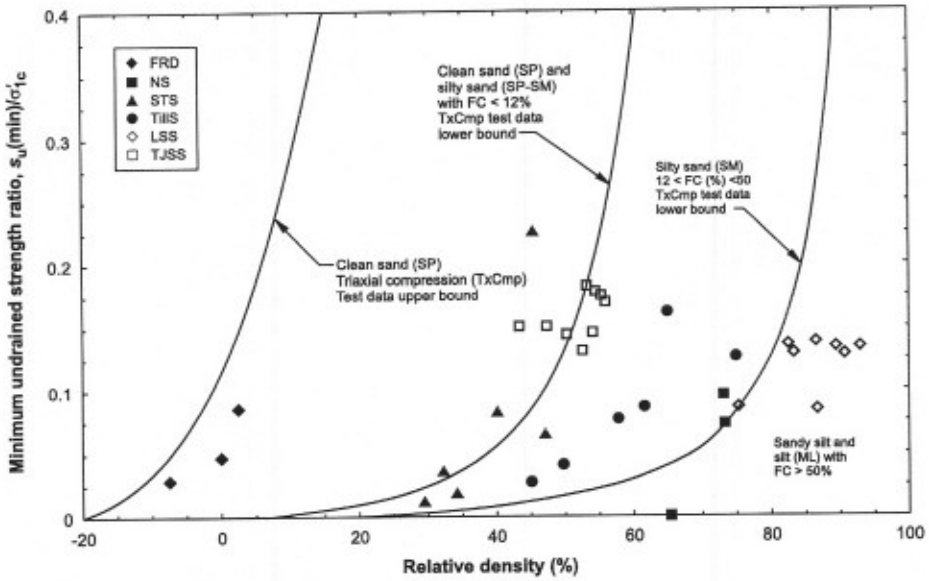

relations proposed by Thevanayagam et al. (1996*a*, 1996*b*). The lower bound relationship for silty sands tested in triaxial compression approaches a vertical asymptote at a relative density of approximately 87%. This vertical asymptote of D_r = 87% falls between those of approximately 77%–97% suggested by Thevanayagam et al. for sands with between 12% and 50% fines content. From Fig. 17, it is evident that silty soils may have very low minimum strength ratios, even at high global relative densities. Lade and Yamamuro (1997), Yamamuro and Lade (1998), Thevanayagam (1998), and others have observed similar low strength behavior in silty sands with high relative densities. This corroborates the conclusion of numerous investigators that relative density is a poor indicator of behavior for silty soils.

Conversion of relative density to penetration resistance

To compare the laboratory data with the relations between liquefied strength ratio and normalized penetration resistance proposed by Olson and Stark (2002), it is necessary to relate relative density to normalized penetration resistance. While some investigators (e.g., Been et al. 1987; Konrad 1998) proposed relations between normalized CPT tip resistance and state parameter, others (e.g., Sladen 1989; Huang et al. 1999) indicated that these relations may not be universally applicable. Although updated correlations include parameters such as shear modulus to improve prediction (Shuttle and Jefferies 1998), this study did not use these relations to estimate normalized penetration resistance. Furthermore, correlations between relative density and normalized penetration resistance based on calibration chamber testing of clean sands may not apply to sands with significant fines content, unless the penetration-induced pore-water pressure is considered (Peterson 1991). For *preliminary* comparison, however, relationships between relative density and normalized penetration resistance developed for clean sands will be used.

Jamiolkowski et al. (1985) proposed the following relation between overburden normalized CPT tip resistance, q_{c1} and relative density (as interpreted by Yoshimine et al. 1999):

$$[4] \qquad q_{c1} = q_{c1N} C_{Pa} = 10^{[(D_r+65)/66]} C_{Pa}$$

where q_{c1N} is a dimensionless normalized CPT tip resistance, and C_{Pa} is a constant equal to 0.1 MPa to convert q_{c1N} to q_{c1} in MPa. This relationship is based on calibration chamber testing of five normally consolidated clean sands. Based on calibration chamber testing of Toyoura sand where penetration-induced pore-water pressure was considered, Yoshimine et al. (1999) suggested a relation proposed by Tatsuoka et al. (1990) between q_{c1N} and relative density as follows:

$$[5] \qquad q_{c1} = q_{c1N} C_{Pa} = 10^{[(D_r+85)/76]} C_{Pa}$$

The q_{c1} values obtained from eqs. [4] and [5] are averaged for use in the following analysis.

Tokimatsu and Seed (1987) proposed the following relation between overburden normalized SPT penetration resistance $(N_1)_{60}$ and relative density:

$$[6] \qquad (N_1)_{60} = 44 D_r^2$$

This relation is based on field density measurements, relative density measurements from samples obtained using in situ freezing, and Meyerhof's (1957) proposed relationship between relative density, vertical effective stress, and SPT blowcount. To account for the effect of grain size on the relation between $(N_1)_{60}$ and relative density observed by Skempton (1986), Kulhawy and Mayne (1990) proposed the following relation:

$$[7] \qquad \frac{(N_1)_{60}}{D_r^2} = 60 + 25 \log D_{50}$$

where D_{50} is median grain diameter in millimetres. This study assumes D_{50} equal to 0.30 mm for clean sands and 0.17 mm for silty sands (as suggested by Stark and Olson

Fig. 18. Comparison of relationships between liquefied strength ratio and normalized CPT tip resistance for laboratory database and flow failure case histories.

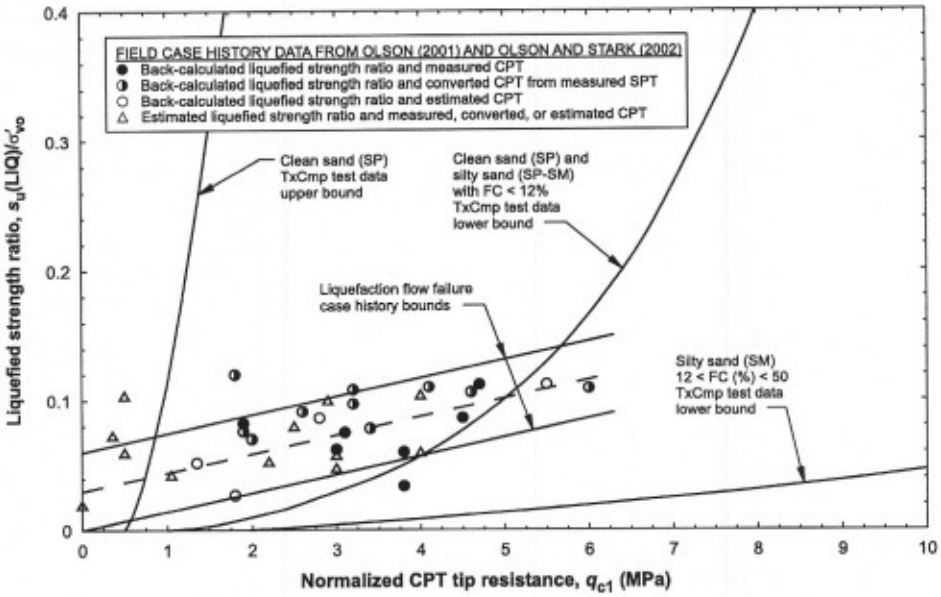

1995). The $(N_1)_{60}$ values obtained from eqs. [6] and [7] also are averaged for use in the following analysis.

Comparison of laboratory and field strength ratio – penetration resistance relationships

Values of relative density for the upper and lower bound D_r – $s_u(\text{min})/\sigma'_{vo}$ relationships for clean and silty sand (Figs. 16 and 17, respectively) were converted to q_{c1} and $(N_1)_{60}$ using the conversions described previously.

Figure 18 presents the upper and lower bound relations between q_{c1} and minimum strength ratio for clean sand and silty sand. Figure 18 includes liquefied strength ratios back-calculated from flow failure case histories and the case history boundaries proposed by Olson and Stark (2002). Similarly, Fig. 19 presents the upper and lower bound relations between $(N_1)_{60}$ and minimum strength ratio. Figure 19 includes the liquefied strength ratios back-calculated from flow failure case histories and the case history boundaries proposed by Olson and Stark (2002).

Generally, the case history data plot between the upper bound relation for clean sands and the lower bound relation for silty sands. The comparisons in Figs. 18 and 19 suggest that the relationships proposed and conclusions made by Olson and Stark (2002) are valid because the laboratory data bracket the back-calculated liquefied strength ratios. Furthermore, the case history data plot near the lower ranges of the laboratory data. This suggests that the soil deposits involved in these flow failures were at least moderately contractive or that some other mechanism (such as mixing) prevented dilation during flow. It should be noted that the laboratory lower bound relationships presented in Figs. 18 and 19 are not intended for use in design. They are used solely to investigate the validity of the relationships proposed by Olson and Stark (2002).

Yoshimine et al. (1999) presented relations between minimum strength ratio, relative density, and dimensionless normalized CPT tip resistance for Toyoura sand. The relations based on triaxial compression tests approach vertical asymptotes at D_r = 32%–36% and a corrected penetration resistance of 3.5–4.0 MPa. These asymptotes plot between the upper and lower bound relationships for clean sands presented in Figs. 16 and 18, respectively. Because the relations presented by Yoshimine et al. are based on one sand (in triaxial compression), they do not appear to be universally applicable to the field case history data. However, these relations for Toyoura sand are in excellent agreement with the clean sand boundaries in Figs. 16 and 18.

Ishihara (1993) presented similar relations between liquefied strength ratio and normalized SPT penetration resistance for Toyoura, Chiba, and Kiyosu sands tested in triaxial compression. These sands approach vertical asymptotes at $(N_1)_{60}$ values of approximately 4.4, 8.5, and 11, respectively. These asymptotes for individual sands plot between the upper and lower bound relationships presented in Fig. 19. Again, the relations presented by Ishihara are based on individual sands (tested in triaxial compression) and do not appear to be universally applicable to the field case history data. However, these relations for Toyoura, Chiba, and Kiyosu sands are in excellent agreement with the clean sand boundaries presented in Fig. 19.

Application of strength ratios in liquefaction analysis

Olson (2001) and Olson and Stark (2003) developed a procedure to evaluate liquefaction of sloping ground that incorporates the yield strength ratio in liquefaction triggering analysis and the liquefied strength ratio in post-triggering analysis. The use of strength ratios for liquefaction analysis allows a designer to incorporate increases in yield and liquefied shear strength that correspond to decreases in void ratio (i.e., an increase in density) resulting from increases in ef-

Fig. 19. Comparison of relationships between liquefied strength ratio and normalized SPT blowcount for laboratory database and flow failure case histories.

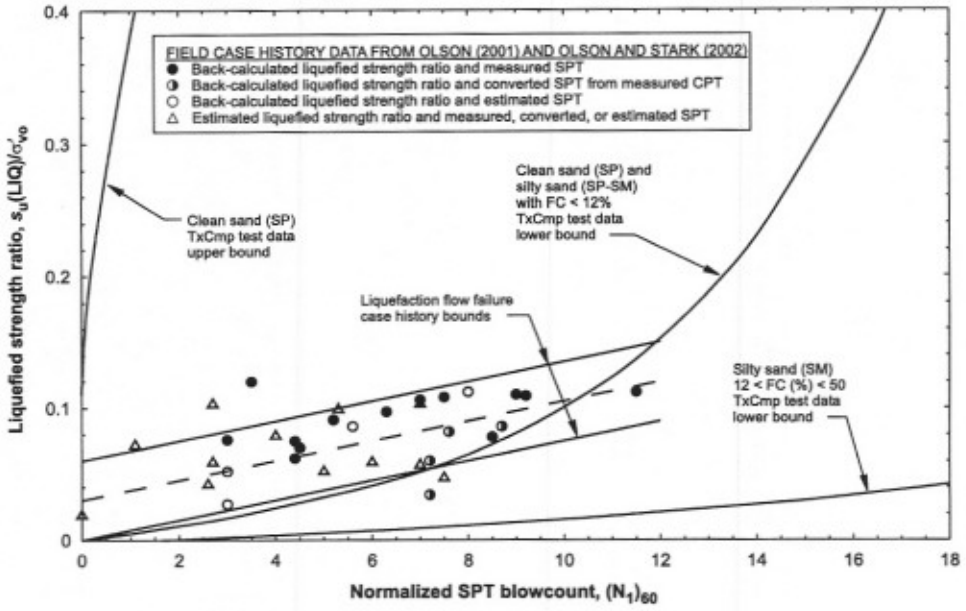

fective confining stress. As illustrated by this study, many sandy soils that are loose enough to be susceptible to flow failure (i.e., contractive) are sufficiently compressible that increases in effective confining stress result in decreases in void ratio that maintain a nearly constant value of state parameter (see Fig. 9). When the state parameter remains constant, yield and liquefied strength ratios are constant for a given sand.

The yield strength ratio basically is equivalent to a yield friction angle, providing the undrained shear strength that is available at various effective stresses prior to the initiation of undrained instability and liquefaction. The yield strength ratio provides a rational means to account for variations in effective stress, state parameter (or void ratio), and grain characteristics via correlation with normalized penetration resistance. Olson and Stark (2003) detail the use of the yield strength ratio in liquefaction analysis of sloping ground, and Olson and Stark (2001) and Olson (2003) illustrate the ease and functionality of its use.

The liquefied strength ratio allows a designer to incorporate variations in liquefied shear strength throughout a zone of liquefaction in a post-triggering stability analysis. Like the yield strength ratio, the liquefied strength ratio provides a rational means to account for variations in effective stress, state parameter (or void ratio), and grain characteristics via correlation with normalized penetration resistance. As discussed by Olson and Stark (2002), increases in liquefied shear strength can be incorporated easily in a post-triggering stability analysis. Additionally, liquefied strength ratios can be used to facilitate liquefaction remediation studies that involve the use of stabilizing berms and soil densification (Olson and Stark 2002).

Conclusions

Laboratory triaxial compression test results from clean sands, silty sands, sandy silts, and silts reported in the literature were collected to validate the strength ratio concepts presented by Olson and Stark (2002, 2003). The database is examined to address the following issues: (*i*) applicability of the yield strength ratio concept; (*ii*) parallelism of consolidation line and steady state line; and (*iii*) applicability of the liquefied strength ratio concept.

The laboratory data exhibit yield strength ratios ranging from 0.29 to 0.42 (with an upper bound of 0.47 at mean effective stresses less than 700 kPa). These bounds correspond to yield friction angles of 16°–23° (with an upper bound of 25°). In comparison, yield strength ratios back-calculated from static flow failure case histories ranged from approximately 0.23 to 0.31. This corresponds to yield friction angles of 13°–17°.

As expected, yield strength ratios back-calculated from static flow failure case histories are smaller than those determined from laboratory triaxial compression tests. This result is expected because the yield shear strength is mobilized at small strains. At small strain, the mobilized strength is a function of the mode of shear, with yield strengths being largest in triaxial compression, smaller in direct simple, rotational, or torsional shear, and likely smallest in triaxial extension. The mode of shear in the zones of liquefaction for most flow failure case histories corresponds approximately to direct simple shear conditions (Olson and Stark 2003), and therefore yield strength ratios back-calculated from the case histories should be smaller than those measured in laboratory triaxial compression tests.

The steady state line and consolidation line are generally parallel for a wide range of effective stresses, steady state line slopes, fines contents, and grain sizes and shapes. Therefore, the liquefied strength ratio should be reasonably constant for a given soil deposited in a consistent manner. In particular, sandy soils with fines contents greater than 12% exhibit nearly parallel slopes of the steady state line and

consolidation line. This parallelism holds for a wide range of effective stresses applicable to many civil engineering structures. As the large majority of flow failure case histories involves sands with some silt, this finding helps explain the relation between liquefied shear strength and vertical effective stress observed for flow failure case histories.

The liquefied strength ratio of individual sands measured in laboratory triaxial compression tests is shown to be inversely proportional to state parameter. For contractive sandy soils (i.e., soils susceptible to flow failure) tested in triaxial compression, the liquefied strength ratio ranges from 0.02 to 0.22 over a wide range of initial major principal effective stresses. Comparison with liquefied strength ratios back-calculated from flow failure case histories shows that the case histories plot near the middle of the laboratory bounds of minimum strength ratio. Assuming that the back-calculated liquefied shear strengths can be directly compared with the minimum strength ratios measured in laboratory tests (which includes some values of quasi-steady-state shear strengths taken as the minimum shear strength), the case histories appear to have state parameters of roughly 0.02 to 0.10.

Lastly, upper and lower bound relationships between laboratory liquefied strength ratios and relative density are presented for relatively clean sands (less than 12% fines content) and silty sands (between 12 and 50% fines content). These relationships were converted to relationships between liquefied strength ratio and normalized SPT and CPT penetration resistance for comparison with field data. The comparisons indicate that the case history data plot between the upper bound relation for clean sands and the lower bound relation for silty sands. This result suggests that the relationships proposed by Olson and Stark (2002) are valid. Furthermore, relations between liquefied strength ratio and normalized penetration resistance (or relative density) based on laboratory testing of one sand (from a given site) can be unconservative for preliminary design involving different sands at other sites.

Acknowledgments

This study was funded by the National Science Foundation (NSF), grant number 97-01785, as part of the Mid-America Earthquake (MAE) Center headquartered at the University of Illinois at Urbana–Champaign. This support is gratefully acknowledged.

References

Arulanandan, K., Seed, H.B., Yogachandran, C., Muraleetharan, K.K., Seed, R.B., and Kabilamany, K. 1993. Centrifuge study on volume changes and dynamic stability of earth dams. Journal of Geotechnical Engineering, ASCE, **119**(11): 1717–1731.

ASTM D4254. Standard test methods for minimum index density and unit weight of soils and calculation of relative density. American Society for Testing and Materials, West Conshohocken, Penn.

Baziar, M.H., and Dobry, R. 1995. Residual strength and large-deformation potential of loose silty sands. Journal of Geotechnical Engineering, ASCE, **121**(12): 896–906.

Been, K., Jefferies, M.G., Crooks, J.H.A., and Rothenburg, L. 1987. The cone penetration test in sands: part II, general inference of state. Géotechnique, **37**(3): 285–299.

Been, K., Jefferies, M.G., and Hachey, J. 1991. The critical state of sands. Géotechnique, **41**(3): 365–381.

Bryant, S.M., Duncan, J.M., and Seed, H.B. 1983. Application of tailings dam flow analyses to field conditions. Report UCB/GT/83-03, Department of Civil Engineering, University of California, Berkeley, Calif.

Canou, J., Bahda, F., Saitta, A., and Dupla, J.C. 1994. Initiation of sand liquefaction under monotonic and cyclic loading. *In* Proceedings of the 13th International Conference on Soil Mechanics and Foundation Engineering, New Delhi, India, 5–10 Jan. 1994. Vol. 3. A.A. Balkema, Rotterdam, The Netherlands. pp. 1297–1300.

Castro, G. 1969. Liquefaction of sands. Ph.D. thesis, Harvard University, Cambridge, Mass.

Castro, G., and Poulos, S.J. 1977. Factors affecting liquefaction and cyclic mobility. Journal of the Geotechnical Engineering Division, ASCE, **103**(GT6): 501–516.

Chillarige, A.V., Robertson, P.K., Morgenstern, N.R., and Christian, H.A. 1997. Evaluation of the in situ state of Fraser River sand. Canadian Geotechnical Journal, **34**: 510–519.

Chu, J. 1995. An experimental examination of the critical state and other similar concepts for granular soils. Canadian Geotechnical Journal, **32**: 1065–1075.

Dennis, N.D. 1988. Influence of specimen preparation techniques and testing procedures on undrained steady state shear strength. *In* Advanced triaxial testing of soil and rock. *Edited by* R.T. Donaghe, R.C. Chaney, and M.L. Silver. American Society for Testing and Materials (ASTM), Special Technical Publication STP 977. pp. 642–654.

Dierichs, D., and Forster, W. 1985. Results of liquefaction tests under static conditions. *In* Proceedings of the 11th International Conference on Soil Mechanics and Foundation Engineering, San Francisco, Calif., 12–16 Aug. 1985. Vol. 2. A.A. Balkema, Rotterdam, The Netherlands. pp. 437–441.

Dyvik, R., and Høeg, K. 1999. Comparison of tests on undisturbed and reconstituted silt and silty sand. *In* Physics and Mechanics of Soil Liquefaction: Proceedings of the International Workshop. *Edited by* P. Lade and J. Yamamuro. Johns Hopkins University, Baltimore, Md., 10–11 Sept. 1998. A.A. Balkema, Rotterdam, The Netherlands.

Fear, C.E., and Robertson, P.K. 1995. Estimating the undrained strength of sand: a theoretical framework. Canadian Geotechnical Journal, **32**: 859–870.

Finn, W.D.L. 1998. Seismic safety of embankment dams: developments in research and practice 1988–1998. *In* Proceedings of the Specialty Conference on Geotechnical Earthquake Engineering and Soil Dynamics III, Seattle. Vol. 2. American Society of Civil Engineers (ASCE), Geotechnical Special Publication 75. pp. 812–853.

Gutierrez, M. 1998. Liquefaction and post-liquefaction behavior of granular soils. *In* Proceedings of the NSF Workshop on Shear Strength of Liquefied Soils, Urbana, Ill., 17–18 April 1997. *Edited by* T.D. Stark, S.M. Olson, S.L. Kramer, and T.L. Youd. University of Illinois at Urbana–Champaign, Urbana, Ill. pp. 88–89 [online]. Available from http://mae.ce.uiuc.edu/Info/Resources.html [cited December 2002].

Hanzawa, H. 1980. Undrained strength and stability analysis for a quick sand. Soils and Foundations, **20**(2): 17–29.

Hanzawa, H., Itoh, Y., and Suzuki, K. 1979. Shear characteristics of a quick sand in the Arabian Gulf. Soils and Foundations, **19**(4): 1–15.

Highter, W.H., and Tobin, R.F. 1980. Flow slides and the undrained

brittleness index of some mine tailings. Engineering Geology, **16**: 71–82.

Highter, W.H., and Vallee, R.P. 1980. The liquefaction of different mine tailings under stress-controlled conditions. Engineering Geology, **16**: 147–150.

Huang, A.-B., Hsu, H.-H., and Chang, J.-W. 1999. The behavior of a compressible silty fine sand. Canadian Geotechnical Journal, **36**: 88–101.

Ishihara, K. 1993. Liquefaction and flow failure during earthquakes. Géotechnique, **43**(3): 351–415.

Jamiolkowski, M., Ladd, C.C., Germaine, J.T., and Lancellotta, R. 1985. New developments in field and laboratory testing of soils. *In* Proceedings of the 11th International Conference on Soil Mechanics and Foundation Engineering, San Francisco, Calif. Vol. 1. A.A. Balkema, Rotterdam, The Netherlands. pp. 57–153.

Kolbuszewski, J.J. 1948. An experimental study of the maximum and minimum porosities of sand. *In* Proceedings of the 4th International Conference on Soil Mechanics and Foundation Engineering, Rotterdam, The Netherlands. pp. 158–165.

Konrad, J.-M. 1990. Minimum undrained strength of two sands. Journal of Geotechnical Engineering, ASCE, **116**(6): 932–947.

Konrad, J.-M. 1993. Undrained response of loosely compacted sands during monotonic and cyclic compression tests. Géotechnique, **43**(1): 69–89.

Konrad, J.-M. 1998. Sand state from cone penetration tests: a framework considering grain crushing stress. Géotechnique, **48**(2): 201–215.

Konrad, J.-M., and Pouliot, N. 1997. Ultimate state of reconstituted and intact samples of deltaic sand. Canadian Geotechnical Journal, **34**: 737–748.

Kramer, S.L., and Seed, H.B. 1988. Initiation of soil liquefaction under static loading condition. Journal of Geotechnical Engineering, ASCE, **114**(4): 412–430.

Kulhawy, F.H., and Mayne, P.W. 1990. Manual on estimating soil properties for foundation design. Electric Power Research Institute EL-6800, Project 1493-6. Electric Power Research Institute, Palo Alto, Calif.

Lade, P.V. 1992. Static instability and liquefaction of loose fine sandy slopes. Journal of Geotechnical Engineering, ASCE, **118**(1): 51–71.

Lade, P.V. 1993. Initiation of static instability in the submarine Nerlerk berm. Canadian Geotechnical Journal, **30**: 895–904.

Lade, P.V., and Yamamuro, J.A. 1997. Effects of nonplastic fines on static liquefaction of sands. Canadian Geotechnical Journal, **34**: 918–928.

Meyerhof, G.G. 1957. Discussion on sand density by spoon penetration. *In* Proceedings of the 4th International Conference on Soil Mechanics and Foundation Engineering. Vol. 3. American Society of Civil Engineers, New York. pp. 110.

Olson, S.M. 2001. Liquefaction analysis of level and sloping ground using field case histories and penetration resistance. Ph.D. thesis, University of Illinois at Urbana–Champaign, Urbana, Ill. [online]. Available from http://pgi-tp.ce.uiuc.edu/olsonwebfiles/olsonweb/index.html [cited December 2002].

Olson, S.M. 2003. Strength ratio-based liquefaction analysis of sloping ground. *In* Proceedings of the 12th Panamerican Conference on Soil Mechanics and Geotechnical Engineering, Boston, Mass., 22–25 June. Paper No. 271.

Olson, S.M., and Stark, T.D. 2001. Liquefaction analysis of Lower San Fernando dam using strength ratios. *In* Proceedings of the 4th International Conference on Recent Advances in Geotechnical Earthquake Engineering and Soil Dynamics, San Diego, Calif., 26–31 March. Paper 4.05.

Olson, S.M., and Stark, T.D. 2002. Liquefied strength ratio from liquefaction flow failure case histories. Canadian Geotechnical Journal, **39**: 629–647.

Olson, S.M., and Stark, T.D. 2003. Yield strength ratio and liquefaction analysis of slopes and embankments. Journal of Geotechnical and Geoenvironmental Engineering, ASCE, **129**(8): 727–737.

Peterson, R.W. 1991. Penetration resistance of fine cohesionless materials. *In* Proceedings of the 1st International Symposium on Calibration Chamber Testing, Potsdam, N.Y., 28–29 June 1991. Elsevier, New York. pp. 315–328.

Pillai, V.S., and Salgado, F.M. 1994. Post-liquefaction stability and deformation analysis of Duncan Dam. Candian Geotechnical Journal, **31**: 967–978.

Pillai, V.S., and Stewart, R.A. 1994. Evaluation of liquefaction potential of foundation soils at Duncan Dam. Canadian Geotechnical Journal, **31**: 951–966.

Poulos, S.J., Castro, G., and France, W. 1985*a*. Liquefaction evaluation procedure. Journal of Geotechnical Engineering, ASCE, **111**(6): 772–792.

Poulos, S.J., Robinsky, E.I., and Keller, T.O. 1985*b*. Liquefaction resistance of thickened tailings. Journal of Geotechnical Engineering, ASCE, **111**(12): 1380–1394.

Riemer, M.F., and Seed, R.B. 1992. Observed effects of testing conditions on the residual strength of loose, saturated sands at large strains. *In* Proceedings of the 4th Japan–U.S. Workshop on Earthquake Resistant Design of Lifeline Facilities and Countermeasures for Soil Liquefaction. *Edited by* M. Hamada and T.D. O'Rourke. Earthquake Engineering Research Center, Technical Report NCEER-92-0019. Vol. 1. National Center for Earthquake Engineering Research (NCEER), Buffalo, N.Y. pp. 223–237.

Riemer, M.F., and Seed, R.B. 1997. Factors affecting apparent position of steady-state line. Journal of Geotechnical and Geoenvironmental Engineering, ASCE, **123**(3): 281–288.

Riemer, M.F., Seed, R.B., Nicholson, P.G., and Jong, H.L. 1990. Steady state testing of loose sands: limiting minimum density. Journal of Geotechnical Engineering, ASCE, **116**(2): 332–337.

Sasitharan, S., Robertson, P.K., Sego, D.C., and Morgenstern, N.R. 1993. Collapse behavior of sand. Canadian Geotechnical Journal, **30**: 569–577.

Sasitharan, S., Robertson, P.K., Sego, D.C., and Morgenstern, N.R. 1994. State-boundary surface for very loose sand and its practical implications. Canadian Geotechnical Journal, **31**: 321–334.

Seed, H.B., Seed, R.B., Harder, L.F., and Jong, H.-L. 1989. Re-evaluation of the Lower San Fernando Dam: Report 2, examination of the post-earthquake slide of February 9, 1971. U.S. Army Corps of Engineers Contract Report GL-89-2. U.S. Army Corps of Engineers Waterways Experiment Station, Vicksburg, Miss.

Shuttle, D., and Jefferies, M. 1998. Dimensionless and unbiased CPT interpretation in sand. International Journal of Numerical and Analytical Methods in Geomechanics, **22**: 351–391.

Skempton, A.W. 1986. Standard penetration test procedures and the effects in sand of overburden pressure, relative density, particle size, ageing, and overconsolidation. Géotechnique, **36**: 425–447.

Sladen, J.A. 1989. Problems with interpretation of sand state from cone penetration test. Géotechnique, **39**(2): 323–332.

Sladen, J.A., and Handford, G. 1987. A potential systematic error in laboratory testing of very loose sands. Canadian Geotechnical Journal, **24**: 462–466.

Sladen, J.A., D'Hollander, R.D., and Krahn, J. 1985. The liquefaction of sands, a collapse surface approach. Canadian Geotechnical Journal, **22**: 564–578.

Stark, T.D., and Olson, S.M. 1995. Liquefaction resistance using CPT and field case histories. Journal of Geotechnical Engineering, ASCE, **121**(12): 856–869.

Takeshita, S., Takeishi, M., and Tamada, K. 1995. Static liquefaction of sands and its liquefaction index. *In* Proceedings of the 1st International Conference on Earthquake Geotechnical Engineering, Tokyo, Japan, 14–16 Nov. 1995. Vol. 1. *Edited by* K. Ishihara. A.A. Balkema, Rotterdam, The Netherlands. pp. 177–182.

Tatsuoka, F., Zhou, S., Sato, T., and Shibuya, S. 1990. Evaluation method of liquefaction potential and its application. *In* Report on seismic hazards on the ground in urban areas. Ministry of Education of Japan, Tokyo. pp. 75–109. [In Japanese.]

Terzaghi, K., Peck, R.B., and Mesri, G. 1996. Soil mechanics in engineering practice. 3rd ed. John Wiley and Sons, Inc., New York.

Thevanayagam, S. 1998. Effect of fines and confining stress on undrained shear strength of silty sands. Journal of Geotechnical and Geoenvironmental Engineering, ASCE, **124**(6): 479–491.

Thevanayagam, S., Ravishankar, K., and Mohan, S. 1996*a*. Steady state strength, relative density and fines content relationship for sands. *In* Proceedings of the Transportation Research Board 75th Annual Meeting, Washington, D.C., 7–11 Jan. 1996.

Thevanayagam, S., Wang, C.C., and Ravishankar, K. 1996*b*. Determination of post-liquefaction strength: steady state vs. residual strength. *In* Proceedings, Uncertainty in the Geologic Environment: From Theory to Practice, Madison, Wisc., 31 July – 3 Aug. 1996. Vol. 2. American Society of Civil Engineers (ASCE), Geotechnical Special Publication 58. pp. 1210–1224.

Tokimatsu, K., and Seed, H.B. 1987. Evaluation of settlements in sands due to earthquake shaking. Journal of Geotechnical Engineering, ASCE, **113**(8): 861–878.

Vaid, Y.P., and Chern, J.C. 1983. Effect of static shear on resistance to liquefaction. Soils and Foundations, **23**(1): 47–60.

Vaid, Y.P., and Chern, J.C. 1985. Cyclic and monotonic undrained response of saturated sands. *In* Advances in the art of testing soils under cyclic conditions. *Edited by* V. Khosla. American Society of Civil Engineers (ASCE), New York. pp. 120–147.

Vaid, Y.P., and Sivathayalan, S. 1996. Static and cyclic liquefaction potential of Fraser Delta sand in simple shear and triaxial tests. Canadian Geotechnical Journal, **33**: 281–289.

Vasquez-Herrera, A., and Dobry, R. 1989. Re-evaluation of the Lower San Fernando Dam: Report 3, the behavior of undrained contractive sand and its effect on seismic liquefaction flow failures of earth structures. U.S. Army Corps of Engineers, Contract Report GL-89-2. U.S. Army Corps of Engineers Waterways Experiment Station, Vicksburg, Miss.

Yamamuro, J.A., and Lade, P.V. 1998. Steady-state concepts and static liquefaction of silty sands. Journal of Geotechnical and Geoenvironmental Engineering, ASCE, **124**(9): 868–877.

Yoshimine, M., and Ishihara, K. 1998. Flow potential of sand during liquefaction. Soils and Foundations, **38**(3): 189–198.

Yoshimine, M., Robertson, P.K., and Wride (Fear), C.E. 1999. Undrained shear strength of clean sands to trigger flow liquefaction. Canadian Geotechnical Journal, **36**: 891–906.

Zlatovic, S., and Ishihara, K. 1995. On the influence of nonplastic fines on residual strength. *In* Proceedings of the 1st International Conference on Earthquake Geotechnical Engineering, Tokyo, Japan, 14–16 Nov. 1995. Vol. 1. *Edited by* K. Ishihara. A.A. Balkema, Rotterdam, The Netherlands. pp. 239–244.